

**SYNTHESIS, CHARACTERIZATION AND  
ANTI-PROLIFERATION STUDY OF SOME  
BENZIMIDAZOLE DERIVATIVES**

**by**

**MOHAMMED HADI SAEED AL-DOUH**

**Thesis submitted in fulfilment of the  
requirements for the degree of  
Doctor of Philosophy**

**2010**

## ACKNOWLEDGEMENT

First and foremost, praise be to ALLAH the Great and Almighty surrounded me under His auspices during my PhD study, in the School of Chemical Sciences, Universiti Sains Malaysia. I would like to express my sincere gratitude to my supervisors, Assoc. Prof. Dr. Hasnah Osman (School of Chemical Sciences, Universiti Sains Malaysia) and Assoc. Prof. Dr. Shafida Abd Hamid (Kulliyah of Science, International Islamic University Malaysia) for their advices, support, direction, and encouragement during experimental work and thesis writing. Their hard work, insights and knowledge have been an inspiration. I would also like to thank to my co-supervisor Dr. Salizawati M. Salhimi (School of Pharmaceutical Sciences, Universiti Sains Malaysia) for her kind assistance whenever I needed it. Her close work with our group has provided great opportunities to further our studies on the application part of our compounds.

I also thank Assoc. Prof. Dr. Mas Rosemal H. M. Haris (School of Chemical Sciences, Universiti Sains Malaysia) and Dr. Peter Springer (Bruker) for their suggestions of the NMR Experiments. I thank Prof. Dr. Hoong K. Fun, Dr. Reza Kia, Miss. Shea L. Ng and Mr. M. M. Rosli for X-ray crystallography analyses, X-ray crystallography Unit, School of Physics, Universiti Sains Malaysia, and Prof. Dr. David S. Larsen and his team for the HRMS analyses, Department of Chemistry, University Otago, Dunedin, New Zealand.

Special thanks are extended to Dr. Amin Malik Shah bin Abdul Majid in the School of Pharmaceutical Sciences, Universiti Sains Malaysia, and to my friends Mr. Hussain M. Ba-Harethah, Mr. Hayder B. Sahib, Mr. Ahmed Faisal, Mr. Muath

H. Helal, Mr. Abd Al-Raheem, Mr. Mahfoudh Al-Musali and Mr. Anas Horani for their help in the technical experiments of MTT assay. I thank my sister, Miss. Hanani (School of Chemical Sciences, Universiti Sains Malaysia) for her translations to Malay language during my study. Additionally, thanks to my uncle Prof. Dr. Mohammed Yaslam Shobrak (College of Sciences, Biology Dept., Taif University) and Prof. Dr. Mohamed Said Fakeh El-Amodi (College of Sciences, Chemistry Dept., Taif University) for their critical reading of this thesis.

I would like to express my thanks to Hadhramout University of Science and Technology (Mukalla, Hadhramout) for the financial scholarship support, School of Chemical Sciences, and to Universiti Sains Malaysia for founded this work by short-term grants: IRPA [304/PKIMIA/636108], IRPA [304/PKIMIA/638007], FRGS [203/PKIMIA/671046], FRGS [304/PKIMIA/638122] and USM-RU-PGRS [1001/PKIMIA/842024].

Finally great thanks to my mother (Khadijah), father (Hadi), brothers (Omar, Hassan, Aymen, Abdullah, Abdulrahman) and sisters (Heba, Hanadi, Hala, Hana, Hajar). I wish to express my special thanks to my wife (Maymonah), son (Hatem) and daughters (Rawan, Rutana, Rulla) for everything that helped me to complete my study.

## **DECLARATION**

The work described in this thesis was undertaken at School of Chemical Sciences, Universiti Sains Malaysia between June 2005 and May 2010 under the supervision of Assoc. Prof. Dr. Hasnah Osman (School of Chemical Sciences, Universiti Sains Malaysia), Assoc. Prof. Dr. Shafida Abd Hamid (Kulliyah of Science, International Islamic University Malaysia) and Dr. Salizawati M. Salhimi (School of Pharmaceutical Sciences, Universiti Sains Malaysia). Except where indicated by reference, it is the original work of the author and has not been submitted in support for another degree or qualification of this or any other university, or institute of higher learning.

## TABLE OF CONTENTS

	<i>Page</i>
Acknowledgement	ii
Table of contents	v
List of tables	xii
List of figures	xv
List of schemes	xxv
List of abbreviations	xxviii
List of appendices	xxxii
Abstrak	xxxiii
Abstract	xxxv
<b>CHAPTER ONE: INTRODUCTION</b>	<b>1</b>
1.1 Schiff bases	1
1.2 Benzimidazoles	4
1.2.1 Substitution at position 2	8
1.2.1.1 Reaction of <i>o</i> -arylene diamines with carboxylic acids	8
1.2.1.2 Reaction of <i>o</i> -arylene diamines with aldehydes	8
1.2.1.3 Reaction of <i>o</i> -arylene diamines with ketones	10
1.2.1.4 Benzimidazole derivatives from $\beta$ -diketone	11
1.2.1.5 Benzimidazoles from the reaction of <i>o</i> -arylene diamines with quinoxalin-2-one derivatives	11
1.2.1.6 Benzimidazoles from <i>o</i> -nitroarylamines	12
1.2.1.7 Benzimidazoles from <i>o</i> -azidoanilines	13
1.2.1.8 Benzimidazoles from amidines	14

1.2.1.9	Benzimidazoles from resin-bound esters	14
1.2.2	1,2-Disubstitution of benzimidazoles	15
1.2.2.1	Benzimidazoles from <i>o</i> -arylene amines	15
1.2.2.2	Benzimidazoles from <i>o</i> -haloaryl amines	17
1.2.2.3	Benzimidazoles from <i>o</i> -nitroaryl amines	17
1.2.2.4	Benzimidazoles from <i>o</i> -halonitrobenzenes	18
1.2.3	Synthesis leading to the formation of both Schiff base and benzimidazoles	19
1.3	Scope of this work	21
1.3.1	The objectives	24
<b>CHAPTER TWO: MATERIALS AND METHODS</b>		<b>25</b>
2.1	Chemicals	25
2.2	Equipments and apparatus for cell proliferation assay	26
2.3	Instrumentation	27
2.4	Synthesis and Characterization	29
2.4.1	2-Benzyloxy-3-methoxybenzaldehyde (benzyl <i>o</i> -vanillin, <b>75</b> )	30
2.4.2	2-Amino- <i>N</i> -(2-hydroxy-3-methoxybenzylidene) benzeneamine ( <b>76</b> ) and 2-amino- <i>N</i> -(2-benzyloxy-3-methoxybenzylidene) benzeneamine ( <b>82</b> )	31
2.4.3	2-(2-Hydroxy-3-methoxyphenyl)-1 <i>H</i> -benzimidazole ( <b>77</b> ), <i>N</i> -1-(2-hydroxy-3-methoxybenzyl)-2-(2-hydroxy-3-methoxyphenyl)-1 <i>H</i> -benzimidazole ( <b>78</b> ), <i>N,N'</i> -bis(2-hydroxy-3-methoxybenzylidene)-1,2-diaminobenzene ( <b>79</b> ), 2-(2-benzyloxy-3-methoxyphenyl)-1 <i>H</i> -benzimidazole ( <b>83</b> ) and <i>N</i> -1-(2-benzyloxy-3-methoxybenzyl)-2-(2-benzyloxy-3-methoxyphenyl)-1 <i>H</i> -benzimidazole ( <b>84</b> )	32
2.4.4	<i>N,N'</i> -Bis(2-hydroxy-3-methoxybenzylidene)-1,3-diaminobenzene ( <b>80</b> ) and <i>N,N'</i> -bis(2-hydroxy-3-methoxybenzylidene)-1,4-diaminobenzene ( <b>81</b> )	34
2.5	Routine cell culture	35

2.6	Cytotoxicity evaluation	36
2.6.1	MTT assay	36
<b>CHAPTER THREE: RESULTS AND DISCUSSION</b>		<b>38</b>
3.1	2-Benzyloxy-3-methoxybenzaldehyde (benzyl <i>o</i> -vanillin) ( <b>75</b> )	38
3.1.1	FTIR Spectroscopy	40
3.1.2	EIMS and HRMS Spectrum	41
3.1.3	<sup>1</sup> H NMR	42
3.1.4	<sup>13</sup> C NMR	45
3.1.5	<sup>1</sup> H- <sup>1</sup> H COSY	47
3.1.6	<sup>1</sup> H- <sup>13</sup> C HMQC	48
3.1.7	<sup>1</sup> H- <sup>13</sup> C HMBC	49
3.1.8	X-ray crystallography	53
3.2	2-Amino- <i>N</i> -(2-hydroxy-3-methoxybenzylidene) benzeneamine ( <b>76</b> )	55
3.2.1	FTIR Spectroscopy	56
3.2.2	HRMS Spectrum	57
3.2.3	<sup>1</sup> H NMR	57
3.2.4	<sup>13</sup> C APT NMR	60
3.2.5	<sup>1</sup> H- <sup>1</sup> H COSY	62
3.2.6	<sup>1</sup> H- <sup>13</sup> C HMQC	64
3.2.7	<sup>1</sup> H- <sup>13</sup> C HMBC	65
3.2.8	X-ray crystallography	66
3.3	2-(2-Hydroxy-3-methoxyphenyl)-1 <i>H</i> -benzimidazole ( <b>77</b> )	69
3.3.1	FTIR Spectroscopy	70
3.3.2	HRMS Spectrum	71

3.3.3	$^1\text{H}$ NMR	72
3.3.4	$^{13}\text{C}$ APT NMR	74
3.3.5	$^1\text{H}$ - $^1\text{H}$ COSY	75
3.3.6	$^1\text{H}$ - $^{13}\text{C}$ HMQC	76
3.3.7	$^1\text{H}$ - $^{13}\text{C}$ HMBC	77
3.3.8	X-ray crystallography	80
3.4	<i>N</i> -1-(2-Hydroxy-3-methoxybenzyl)-2-(2-hydroxy-3-methoxyphenyl)-1 <i>H</i> -benzimidazole ( <b>78</b> )	82
3.4.1	FTIR Spectroscopy	82
3.4.2	HRMS Spectrum	83
3.4.3	$^1\text{H}$ NMR	84
3.4.4	$^{13}\text{C}$ APT NMR	86
3.4.5	$^1\text{H}$ - $^1\text{H}$ COSY	87
3.4.6	$^1\text{H}$ - $^{13}\text{C}$ HMQC	89
3.4.7	$^1\text{H}$ - $^{13}\text{C}$ HMBC	90
3.4.8	X-ray crystallography	92
3.5	<i>N,N'</i> -Bis(2-hydroxy-3-methoxybenzylidene)-1,2-diaminobenzene ( <b>79</b> )	97
3.5.1	HRMS Spectrum	97
3.5.2	$^1\text{H}$ NMR	98
3.5.3	$^{13}\text{C}$ NMR	99
3.5.4	$^1\text{H}$ - $^1\text{H}$ COSY	100
3.5.5	$^1\text{H}$ - $^{13}\text{C}$ HMQC	102
3.5.6	$^1\text{H}$ - $^{13}\text{C}$ HMBC	102
3.5.7	X-ray crystallography	104
3.6	<i>N,N'</i> -Bis(2-hydroxy-3-methoxybenzylidene)-1,3-diaminobenzene ( <b>80</b> )	107

3.6.1	HRMS Spectrum	108
3.6.2	<sup>1</sup> H NMR	108
3.6.3	<sup>13</sup> C NMR	109
3.6.4	<sup>1</sup> H- <sup>1</sup> H COSY	111
3.6.5	<sup>1</sup> H- <sup>13</sup> C HMQC	112
3.6.6	<sup>1</sup> H- <sup>13</sup> C HMBC	113
3.6.7	X-ray crystallography	115
3.7	<i>N,N'</i> -Bis(2-hydroxy-3-methoxybenzylidene)-1,4-diaminobenzene ( <b>81</b> )	118
3.7.1	FTIR Spectroscopy	119
3.7.2	HRMS Spectrum	120
3.7.3	<sup>1</sup> H NMR	121
3.7.4	<sup>13</sup> C NMR	121
3.7.5	<sup>1</sup> H- <sup>1</sup> H COSY	123
3.7.6	<sup>1</sup> H- <sup>13</sup> C HMQC	124
3.7.7	<sup>1</sup> H- <sup>13</sup> C HMBC	125
3.7.8	X-ray crystallography	127
3.7.9	The cytotoxicity of bis-Schiff bases <b>79</b> , <b>80</b> and <b>81</b>	129
3.8	2-Amino- <i>N</i> -(2-benzyloxy-3-methoxybenzylidene) benzeneamine ( <b>82</b> )	131
3.8.1	FTIR Spectroscopy	132
3.8.2	HRMS Spectrum	134
3.8.3	<sup>1</sup> H NMR	135
3.8.4	<sup>13</sup> C NMR	136
3.8.5	<sup>1</sup> H- <sup>1</sup> H COSY	138
3.8.6	<sup>1</sup> H- <sup>13</sup> C HMQC	139
3.8.7	<sup>1</sup> H- <sup>13</sup> C HMBC	140

3.8.8	X-ray crystallography	143
3.9	2-(2-Benzyloxy-3-methoxyphenyl)-1 <i>H</i> -benzimidazole ( <b>83</b> )	145
3.9.1	FTIR Spectroscopy	147
3.9.2	EIMS and HRMS Spectrum	148
3.9.3	<sup>1</sup> H NMR	150
3.9.4	<sup>13</sup> C NMR	152
3.9.5	<sup>1</sup> H- <sup>1</sup> H COSY	155
3.9.6	<sup>1</sup> H- <sup>13</sup> C HMQC	158
3.9.7	<sup>1</sup> H- <sup>13</sup> C HMBC	159
3.9.8	X-ray crystallography	161
3.10	<i>N</i> -1-(2-Benzyloxy-3-methoxybenzyl)-2-(2-benzyloxy-3-methoxyphenyl)-1 <i>H</i> -benzimidazole ( <b>84</b> )	164
3.10.1	FTIR Spectroscopy	167
3.10.2	HRMS Spectrum	168
3.10.3	<sup>1</sup> H NMR	169
3.10.4	<sup>13</sup> C NMR	171
3.10.5	<sup>1</sup> H- <sup>1</sup> H COSY	173
3.10.6	<sup>1</sup> H- <sup>13</sup> C HMQC	174
3.10.7	<sup>1</sup> H- <sup>13</sup> C HMBC	175
3.11	Potential biological activity of benzimidazoles <b>77</b> , <b>78</b> , <b>83</b> and <b>84</b>	179
3.11.1	Introduction	179
3.11.2	Cytotoxicity effect of benzimidazoles <b>77</b> , <b>78</b> , <b>83</b> and <b>84</b> on MCF-7 breast cancer cell line and HCT-116 colon cancer cell line	181
	<b>CHAPTER FOUR: CONCLUSION</b>	<b>188</b>
	<b>REFERENCES</b>	<b>190</b>

<b>APPENDICES</b>	<b>207</b>
<b>LIST OF PUBLICATIONS</b>	<b>225</b>
A. International refereed journals	225
B. Papers presented at international and national conferences	227

## LIST OF TABLES

		<i>Page</i>
<b>Table 3.1</b>	Benylation of <i>o</i> -vanillin (1.0 equiv.) by benzyl halides (X) produced <i>via</i> Scheme 3.1	40
<b>Table 3.2</b>	FTIR spectral data of compound <b>75</b> (cm <sup>-1</sup> )	41
<b>Table 3.3</b>	<sup>1</sup> H and <sup>13</sup> C NMR chemical shifts (ppm) and coupling constants (Hz) of <b>75</b> in CDCl <sub>3</sub> and acetone- <i>d</i> <sub>6</sub>	46
<b>Table 3.4</b>	2D <sup>1</sup> H- <sup>1</sup> H COSY, <sup>1</sup> H- <sup>13</sup> C HMQC and HMBC correlations for <b>75</b> in CDCl <sub>3</sub> and acetone- <i>d</i> <sub>6</sub>	52
<b>Table 3.5</b>	Hydrogen bond geometry of <b>75</b> (Å, °)	54
<b>Table 3.6</b>	FTIR spectral data of <b>76</b> (cm <sup>-1</sup> )	56
<b>Table 3.7</b>	<sup>1</sup> H and <sup>13</sup> C APT NMR chemical shifts (ppm) and coupling constants (Hz) of <b>76</b> in CDCl <sub>3</sub>	62
<b>Table 3.8</b>	2D <sup>1</sup> H- <sup>1</sup> H COSY, <sup>1</sup> H- <sup>13</sup> C HMQC and HMBC correlations for <b>76</b> in CDCl <sub>3</sub>	66
<b>Table 3.9</b>	Hydrogen bond geometry of <b>76</b> (Å, °)	68
<b>Table 3.10</b>	FTIR spectral data of benzimidazole <b>77</b> (cm <sup>-1</sup> )	70
<b>Table 3.11</b>	<sup>1</sup> H and <sup>13</sup> C APT NMR chemical shifts (ppm) and coupling constants (Hz) of <b>77</b> in CD <sub>3</sub> OD	75
<b>Table 3.12</b>	2D <sup>1</sup> H- <sup>1</sup> H COSY, <sup>1</sup> H- <sup>13</sup> C HMQC and HMBC correlations for <b>77</b> in CD <sub>3</sub> OD	79
<b>Table 3.13</b>	Hydrogen bond geometry of <b>77</b> (Å, °)	81
<b>Table 3.14</b>	FTIR spectral data of benzimidazole <b>78</b> (cm <sup>-1</sup> )	83
<b>Table 3.15</b>	<sup>1</sup> H and <sup>13</sup> C APT NMR chemical shifts (ppm) and coupling constants (Hz) of <b>78</b> in CDCl <sub>3</sub>	87
<b>Table 3.16</b>	2D <sup>1</sup> H- <sup>1</sup> H COSY, <sup>1</sup> H- <sup>13</sup> C HMQC and HMBC correlations for <b>78</b> in CDCl <sub>3</sub>	92
<b>Table 3.17</b>	Hydrogen bond geometry of <b>78A</b> (Å, °)	96
<b>Table 3.18</b>	Hydrogen bond geometry of <b>78B</b> (Å, °)	96

<b>Table 3.19</b>	$^1\text{H}$ and $^{13}\text{C}$ NMR chemical shifts (ppm) and coupling constants (Hz) of <b>79</b> in $\text{CDCl}_3$	100
<b>Table 3.20</b>	2D $^1\text{H}$ - $^1\text{H}$ COSY, $^1\text{H}$ - $^{13}\text{C}$ HMQC and HMBC correlations for <b>79</b> in $\text{CDCl}_3$	104
<b>Table 3.21</b>	Hydrogen bond geometry of <b>79</b> ( $\text{\AA}$ , $^\circ$ )	106
<b>Table 3.22</b>	$^1\text{H}$ and $^{13}\text{C}$ NMR chemical shifts (ppm) and coupling constants (Hz) of <b>80</b> in $\text{CDCl}_3$	110
<b>Table 3.23</b>	2D $^1\text{H}$ - $^1\text{H}$ COSY, $^1\text{H}$ - $^{13}\text{C}$ HMQC and HMBC correlations for <b>80</b> in $\text{CDCl}_3$	114
<b>Table 3.24</b>	Hydrogen bond geometry of <b>80</b> ( $\text{\AA}$ , $^\circ$ )	117
<b>Table 3.25</b>	FTIR spectral data of bis-Schiff bases <b>79</b> , <b>80</b> and <b>81</b> ( $\text{cm}^{-1}$ )	120
<b>Table 3.26</b>	$^1\text{H}$ and $^{13}\text{C}$ NMR chemical shifts (ppm) and coupling constants (Hz) of <b>81</b> in $\text{CDCl}_3$	122
<b>Table 3.27</b>	2D $^1\text{H}$ - $^1\text{H}$ COSY, $^1\text{H}$ - $^{13}\text{C}$ HMQC and HMBC correlations for <b>81</b> in $\text{CDCl}_3$	127
<b>Table 3.28</b>	Hydrogen bond geometry of <b>81</b> ( $\text{\AA}$ , $^\circ$ )	129
<b>Table 3.29</b>	The $\text{IC}_{50}$ values ( $\mu\text{g/mL}$ ) of bis-Schiff bases <b>79</b> , <b>80</b> and <b>81</b> against MCF-7, T-47D, HepG2, K562 and U937	130
<b>Table 3.30</b>	FTIR spectral data of <b>82</b> ( $\text{cm}^{-1}$ )	133
<b>Table 3.31</b>	$^1\text{H}$ and $^{13}\text{C}$ NMR chemical shifts (ppm) and coupling constants (Hz) of <b>82</b> in $\text{CDCl}_3$	137
<b>Table 3.32</b>	2D $^1\text{H}$ - $^1\text{H}$ COSY, $^1\text{H}$ - $^{13}\text{C}$ HMQC and HMBC correlations for <b>82</b> in $\text{CDCl}_3$	142
<b>Table 3.33</b>	Hydrogen bond geometry of <b>82</b> ( $\text{\AA}$ , $^\circ$ )	144
<b>Table 3.34</b>	FTIR spectral data of benzimidazole <b>83</b> ( $\text{cm}^{-1}$ )	148
<b>Table 3.35</b>	$^1\text{H}$ and $^{13}\text{C}$ NMR chemical shifts (ppm) and coupling constants (Hz) of <b>83</b> in $\text{CDCl}_3$ and acetone- $d_6$	155
<b>Table 3.36</b>	2D $^1\text{H}$ - $^1\text{H}$ COSY, $^1\text{H}$ - $^{13}\text{C}$ HMQC and HMBC correlations for <b>83</b> in $\text{CDCl}_3$ and acetone- $d_6$	161
<b>Table 3.37</b>	Hydrogen bond geometry of <b>83</b> ( $\text{\AA}$ , $^\circ$ )	163
<b>Table 3.38</b>	FTIR spectral data of benzimidazole <b>84</b> ( $\text{cm}^{-1}$ )	168

<b>Table 3.39</b>	$^1\text{H}$ and $^{13}\text{C}$ NMR chemical shifts (ppm) and coupling constants (Hz) of <b>84</b> in acetone- $d_6$	172
<b>Table 3.40</b>	2D $^1\text{H}$ - $^1\text{H}$ COSY, $^1\text{H}$ - $^{13}\text{C}$ HMQC and HMBC correlations for <b>84</b> in acetone- $d_6$	178
<b>Table 3.41</b>	Several benzimidazoles and their $\text{IC}_{50}$ ( $\mu\text{M}$ ) against MCF-7	180
<b>Table 3.42</b>	The $\text{IC}_{50}$ values of the benzimidazoles <b>77</b> , <b>78</b> , <b>83</b> and <b>84</b> against MCF-7 and HCT-116	187

## LIST OF FIGURES

		<i>Page</i>
<b>Figure 1.1</b>	The general formula of Schiff base or imine	1
<b>Figure 1.2</b>	Some symmetrical and unsymmetrical bis-Schiff bases	2
<b>Figure 1.3</b>	Intramolecular hydrogen bond	4
<b>Figure 1.4</b>	The benzimidazole ring	4
<b>Figure 1.5</b>	The benzimidazole ring in the chemical structure of vitamin B <sub>12</sub> , <b>7</b>	5
<b>Figure 1.6</b>	The chemical structures of some benzimidazole derivatives evaluated medicinally	6
<b>Figure 1.7</b>	Some benzimidazole derivatives evaluated for biological activity	7
<b>Figure 1.8</b>	Benzimidazole derivatives evaluated against cancer cell lines	21
<b>Figure 1.9</b>	Structure of benzyl <i>o</i> -vanillin <b>75</b>	22
<b>Figure 1.10</b>	Structures of 2-amino- <i>N</i> -benzylidene benzeneamines <b>76</b> and <b>82</b>	22
<b>Figure 1.11</b>	Structures of bis-Schiff bases <b>79</b> , <b>80</b> and <b>81</b>	23
<b>Figure 1.12</b>	Structures of benzimidazoles <b>77</b> , <b>78</b> , <b>83</b> and <b>84</b>	23
<b>Figure 3.1</b>	The chemical structure and the numbering scheme of <b>75</b>	40
<b>Figure 3.2</b>	FTIR spectrum of <b>75</b>	41
<b>Figure 3.3</b>	EIMS spectrum of <b>75</b>	42
<b>Figure 3.4</b>	HRMS spectrum of <b>75</b>	42
<b>Figure 3.5</b>	<sup>1</sup> H NMR spectrum of <b>75</b> in CDCl <sub>3</sub>	43
<b>Figure 3.6</b>	<sup>1</sup> H NMR spectrum of <b>75</b> in acetone- <i>d</i> <sub>6</sub>	44
<b>Figure 3.7</b>	The correlation between aldehydic proton and H <sub>5</sub> in <b>75</b>	44
<b>Figure 3.8</b>	<sup>13</sup> C NMR spectrum of <b>75</b> in CDCl <sub>3</sub>	45

<b>Figure 3.9</b>	$^{13}\text{C}$ NMR spectrum of <b>75</b> in acetone- $d_6$	46
<b>Figure 3.10</b>	$^1\text{H}$ - $^1\text{H}$ COSY NMR spectrum of <b>75</b> in acetone- $d_6$	47
<b>Figure 3.11</b>	The correlations observed in COSY spectrum of <b>75</b>	48
<b>Figure 3.12</b>	$^1\text{H}$ - $^{13}\text{C}$ HMQC NMR spectrum of <b>75</b> in $\text{CDCl}_3$	48
<b>Figure 3.13</b>	$^1\text{H}$ - $^{13}\text{C}$ HMQC NMR spectrum of <b>75</b> in acetone- $d_6$	49
<b>Figure 3.14</b>	$^1\text{H}$ - $^{13}\text{C}$ HMBC NMR spectrum of <b>75</b> in $\text{CDCl}_3$	50
<b>Figure 3.15</b>	$^1\text{H}$ - $^{13}\text{C}$ HMBC NMR spectrum of <b>75</b> in acetone- $d_6$	50
<b>Figure 3.16</b>	The correlations observed in HMBC spectrum of <b>75</b>	51
<b>Figure 3.17</b>	The crystal structure of <b>75</b> showing 50% probability displacement ellipsoids and the atomic numbering. The dashed lines indicate intramolecular hydrogen bonds	53
<b>Figure 3.18</b>	The crystal packing of <b>75</b> , viewed down the $b$ axis. Intermolecular hydrogen bonds are shown as dashed lines	54
<b>Figure 3.19</b>	The chemical structure and the numbering scheme of <b>76</b>	56
<b>Figure 3.20</b>	FTIR spectrum of <b>76</b>	56
<b>Figure 3.21</b>	HRMS spectrum of <b>76</b>	57
<b>Figure 3.22</b>	The proposed structures of the prominent peak of <b>76</b>	57
<b>Figure 3.23</b>	$^1\text{H}$ NMR spectrum of <b>76</b> in $\text{CDCl}_3$	58
<b>Figure 3.24</b>	$^1\text{H}$ NMR spectrum of <b>76</b> in $\text{CD}_2\text{Cl}_2$	59
<b>Figure 3.25</b>	$^1\text{H}$ NMR spectrum of <b>76</b> in acetone- $d_6$	59
<b>Figure 3.26</b>	The possibility of intramolecular hydrogen bonding in <b>76</b>	60
<b>Figure 3.27</b>	$^{13}\text{C}$ APT NMR spectrum of <b>76</b> in $\text{CDCl}_3$	61
<b>Figure 3.28</b>	$^{13}\text{C}$ APT NMR spectrum of <b>76</b> in $\text{CD}_2\text{Cl}_2$	61
<b>Figure 3.29</b>	$^1\text{H}$ - $^1\text{H}$ COSY NMR spectrum of <b>76</b> in $\text{CDCl}_3$	63
<b>Figure 3.30</b>	$^1\text{H}$ - $^1\text{H}$ COSY NMR spectrum of <b>76</b> in acetone- $d_6$	63
<b>Figure 3.31</b>	$^1\text{H}$ - $^1\text{H}$ COSY NMR spectrum of <b>76</b> in $\text{CD}_2\text{Cl}_2$	63

<b>Figure 3.32</b>	$^1\text{H}$ - $^{13}\text{C}$ HMQC NMR spectrum of <b>76</b> in $\text{CDCl}_3$	64
<b>Figure 3.33</b>	$^1\text{H}$ - $^{13}\text{C}$ HMQC NMR spectrum of <b>76</b> in $\text{CD}_2\text{Cl}_2$	64
<b>Figure 3.34</b>	$^1\text{H}$ - $^{13}\text{C}$ HMBC NMR spectrum of <b>76</b> in $\text{CDCl}_3$	65
<b>Figure 3.35</b>	The correlations observed in HMBC spectrum of <b>76</b> in $\text{CDCl}_3$	65
<b>Figure 3.36</b>	The molecular structure of <b>76</b> showing 50% probability displacement ellipsoids and the atomic numbering. The dashed lines indicate intramolecular hydrogen bonds	67
<b>Figure 3.37</b>	The zigzag stacking arrangement of <b>76</b> viewed along the <i>b</i> axis. Hydrogen bonds are drawn as dashed lines	67
<b>Figure 3.38</b>	The crystal packing of <b>76</b> , viewed down the <i>c</i> axis showing the molecular stacking. Hydrogen bonds are drawn as dashed lines	68
<b>Figure 3.39</b>	The chemical structure and the numbering scheme of <b>77</b>	70
<b>Figure 3.40</b>	FTIR spectrum of <b>77</b>	70
<b>Figure 3.41</b>	HRMS spectrum of <b>77</b>	71
<b>Figure 3.42</b>	The proposed structures of the basic and prominent peaks in HRMS spectrum of <b>77</b>	71
<b>Figure 3.43</b>	$^1\text{H}$ NMR spectrum of <b>77</b> in $\text{CD}_3\text{OD}$	72
<b>Figure 3.44</b>	$^1\text{H}$ NMR spectrum of <b>77</b> in acetone- $d_6$	73
<b>Figure 3.45</b>	$^1\text{H}$ NMR spectrum of <b>77</b> in $\text{DMSO}-d_6$	73
<b>Figure 3.46</b>	$^{13}\text{C}$ APT NMR spectrum of <b>77</b> in $\text{CD}_3\text{OD}$	74
<b>Figure 3.47</b>	$^1\text{H}$ - $^1\text{H}$ COSY NMR spectrum of <b>77</b> in $\text{CD}_3\text{OD}$	76
<b>Figure 3.48</b>	Aromatic protons in $^1\text{H}$ - $^1\text{H}$ COSY NMR spectrum of <b>77</b> in $\text{CD}_3\text{OD}$	76
<b>Figure 3.49</b>	$^1\text{H}$ - $^{13}\text{C}$ HMQC NMR spectrum of <b>77</b> in $\text{CD}_3\text{OD}$	77
<b>Figure 3.50</b>	Aromatic protons and carbons in $^1\text{H}$ - $^{13}\text{C}$ HMQC NMR spectrum of <b>76</b> in $\text{CD}_3\text{OD}$	77
<b>Figure 3.51</b>	$^1\text{H}$ - $^{13}\text{C}$ HMBC NMR spectrum of <b>77</b> in $\text{CD}_3\text{OD}$	78

<b>Figure 3.52</b>	Aromatic protons and carbons in $^1\text{H}$ - $^{13}\text{C}$ HMBC NMR spectrum of <b>76</b> in $\text{CD}_3\text{OD}$	78
<b>Figure 3.53</b>	The correlations observed in HMBC spectrum of <b>77</b>	79
<b>Figure 3.54</b>	The crystal structure of <b>77</b> showing 50% probability displacement ellipsoids and the atomic numbering. The dashed line indicates intramolecular hydrogen bonds	80
<b>Figure 3.55</b>	The crystal packing of <b>77</b> , viewed down the <i>b</i> axis. Intermolecular hydrogen bonds are shown as dashed lines	81
<b>Figure 3.56</b>	The chemical structure and the numbering scheme of <b>78</b>	82
<b>Figure 3.57</b>	FTIR spectrum of <b>78</b>	83
<b>Figure 3.58</b>	HRMS spectrum of <b>78</b>	84
<b>Figure 3.59</b>	The proposed structures of the basic and prominent peaks in HRMS spectrum of <b>78</b>	84
<b>Figure 3.60</b>	$^1\text{H}$ NMR spectrum of <b>78</b> in $\text{CDCl}_3$	85
<b>Figure 3.61</b>	$^{13}\text{C}$ APT NMR spectrum of <b>78</b> in $\text{CDCl}_3$	86
<b>Figure 3.62</b>	$^1\text{H}$ - $^1\text{H}$ COSY NMR spectrum of <b>78</b> in $\text{CDCl}_3$	88
<b>Figure 3.63</b>	Aromatic protons in $^1\text{H}$ - $^1\text{H}$ COSY NMR spectrum of <b>78</b>	88
<b>Figure 3.64</b>	The correlations observed in COSY spectrum of <b>78</b>	88
<b>Figure 3.65</b>	$^1\text{H}$ - $^{13}\text{C}$ HMQC NMR spectrum of <b>78</b> in $\text{CDCl}_3$	89
<b>Figure 3.66</b>	Aromatic protons and carbons in $^1\text{H}$ - $^{13}\text{C}$ HMQC NMR spectrum of <b>78</b>	90
<b>Figure 3.67</b>	$^1\text{H}$ - $^{13}\text{C}$ HMBC NMR spectrum of <b>78</b> in $\text{CDCl}_3$	91
<b>Figure 3.68</b>	The correlations observed in HMBC spectrum of <b>78</b>	91
<b>Figure 3.69</b>	The molecular structure of <b>78A</b> showing 50% probability displacement ellipsoids and the atomic numbering. The disordered methanol solvent molecules were omitted for clarity. Intramolecular hydrogen bonds are drawn as dashed lines	93
<b>Figure 3.70</b>	The conversion of <b>78B</b> from <b>78A</b>	94

<b>Figure 3.71</b>	The molecular structure of <b>78B</b> showing 50% probability displacement ellipsoids and the atomic numbering. Intramolecular H bonds are shown as dashed lines	95
<b>Figure 3.72</b>	Part of the crystal structure of <b>78B</b> viewed along the <i>a</i> -axis showing 1-D extended chains along the <i>c</i> -axis. Intermolecular interactions are drawn as dashed lines	95
<b>Figure 3.73</b>	The chemical structure and the numbering scheme of <b>79</b>	97
<b>Figure 3.74</b>	The HRMS spectrum of <b>79</b>	97
<b>Figure 3.75</b>	The proposed structures of the prominent peak in HRMS spectrum of <b>79</b>	98
<b>Figure 3.76</b>	<sup>1</sup> H NMR spectrum of <b>79</b> in CDCl <sub>3</sub>	98
<b>Figure 3.77</b>	<sup>13</sup> C NMR spectrum of <b>79</b> in CDCl <sub>3</sub>	99
<b>Figure 3.78</b>	<sup>1</sup> H- <sup>1</sup> H COSY NMR spectrum of <b>79</b> in CDCl <sub>3</sub>	101
<b>Figure 3.79</b>	<sup>1</sup> H- <sup>1</sup> H COSY NMR spectrum of aromatic protons of <b>79</b>	101
<b>Figure 3.80</b>	The correlations observed in COSY spectrum of <b>79</b>	101
<b>Figure 3.81</b>	<sup>1</sup> H- <sup>13</sup> C HMQC NMR spectrum of <b>79</b> in CDCl <sub>3</sub>	102
<b>Figure 3.82</b>	<sup>1</sup> H- <sup>13</sup> C HMBC NMR spectrum of <b>79</b> in CDCl <sub>3</sub>	103
<b>Figure 3.83</b>	The correlations observed in HMBC spectrum of <b>79</b>	103
<b>Figure 3.84</b>	The crystal structure of <b>79</b> showing 50% probability displacement ellipsoids and the atomic numbering. The dashed lines indicate intramolecular hydrogen bonds	105
<b>Figure 3.85</b>	The crystal packing of <b>79</b> , viewed down the <i>b</i> axis. Intramolecular hydrogen bonds are shown as dashed lines	105
<b>Figure 3.86</b>	The chemical structure and the numbering scheme of <b>80</b>	107
<b>Figure 3.87</b>	HRMS spectrum of <b>80</b>	108
<b>Figure 3.88</b>	The proposed structures of the prominent peak of <b>80</b>	108
<b>Figure 3.89</b>	<sup>1</sup> H NMR spectrum of <b>80</b> in CDCl <sub>3</sub>	109
<b>Figure 3.90</b>	<sup>13</sup> C NMR spectrum of <b>80</b> in CDCl <sub>3</sub>	110
<b>Figure 3.91</b>	<sup>1</sup> H- <sup>1</sup> H COSY NMR spectrum of <b>80</b> in CDCl <sub>3</sub>	111

<b>Figure 3.92</b>	$^1\text{H}$ - $^1\text{H}$ COSY NMR spectrum of aromatic protons of <b>80</b>	111
<b>Figure 3.93</b>	The correlations observed in COSY spectrum of <b>80</b>	112
<b>Figure 3.94</b>	$^1\text{H}$ - $^{13}\text{C}$ HMQC NMR spectrum of <b>80</b> in $\text{CDCl}_3$	112
<b>Figure 3.95</b>	$^1\text{H}$ - $^{13}\text{C}$ HMBC NMR spectrum of <b>80</b> in $\text{CDCl}_3$	113
<b>Figure 3.96</b>	Aromatic protons and carbons in $^1\text{H}$ - $^{13}\text{C}$ HMBC NMR spectrum of <b>80</b>	114
<b>Figure 3.97</b>	The correlations observed in HMBC spectrum of <b>80</b>	114
<b>Figure 3.98</b>	The crystal structure of <b>80</b> showing 50% probability displacement ellipsoids and the atomic numbering. The dashed lines indicate intramolecular hydrogen bonds	115
<b>Figure 3.99</b>	The crystal packing of <b>80</b> , viewed down the <i>a</i> axis. Intramolecular hydrogen bonds are shown as dashed lines	116
<b>Figure 3.100</b>	The chemical structure and the numbering scheme of <b>81</b>	118
<b>Figure 3.101</b>	FTIR spectra of a) <b>79</b> , b) <b>80</b> and c) <b>81</b>	119
<b>Figure 3.102</b>	HRMS spectrum of <b>81</b>	120
<b>Figure 3.103</b>	The proposed structures of the prominent peak of <b>81</b>	120
<b>Figure 3.104</b>	$^1\text{H}$ NMR spectrum of <b>81</b> in $\text{CDCl}_3$	121
<b>Figure 3.105</b>	$^{13}\text{C}$ NMR spectrum of <b>81</b> in $\text{CDCl}_3$	122
<b>Figure 3.106</b>	$^1\text{H}$ - $^1\text{H}$ COSY NMR spectrum of <b>81</b> in $\text{CDCl}_3$	123
<b>Figure 3.107</b>	$^1\text{H}$ - $^1\text{H}$ COSY NMR spectrum of aromatic protons of <b>81</b>	123
<b>Figure 3.108</b>	The correlations observed in COSY spectrum of <b>81</b>	124
<b>Figure 3.109</b>	$^1\text{H}$ - $^{13}\text{C}$ HMQC NMR spectrum of <b>81</b> in $\text{CDCl}_3$	124
<b>Figure 3.110</b>	$^1\text{H}$ - $^{13}\text{C}$ HMBC NMR spectrum of <b>81</b> in $\text{CDCl}_3$	125
<b>Figure 3.111</b>	Aromatic protons and carbons in $^1\text{H}$ - $^{13}\text{C}$ HMBC NMR spectrum of <b>81</b>	126
<b>Figure 3.112</b>	The correlations observed in HMBC spectrum of <b>81</b>	126

<b>Figure 3.113</b>	The molecular structure of <b>81</b> showing 50% probability displacement ellipsoids and the atomic numbering [symmetry code of unlabelled atoms $-x + 1, -y, -z + 2$ ]. Intramolecular H bonds are drawn as dashed lines	128
<b>Figure 3.114</b>	The crystal packing of <b>81</b> , viewed down the <i>c</i> axis showing of molecules along the <i>c</i> axis. Intramolecular hydrogen bonds are shown as dashed lines	128
<b>Figure 3.115</b>	The chemical structure and the numbering scheme of <b>82</b>	131
<b>Figure 3.116</b>	FTIR spectrum of <b>82</b>	133
<b>Figure 3.117</b>	The possibility of intramolecular hydrogen bonding in <b>82</b>	133
<b>Figure 3.118</b>	High-resolution mass spectrum of <b>82</b>	134
<b>Figure 3.119</b>	The proposed structures of the basic peaks of <b>82</b>	134
<b>Figure 3.120</b>	$^1\text{H}$ NMR spectrum of <b>82</b> in $\text{CDCl}_3$	135
<b>Figure 3.121</b>	$^{13}\text{C}$ NMR spectrum of <b>82</b> in $\text{CDCl}_3$	137
<b>Figure 3.122</b>	$^1\text{H}$ - $^1\text{H}$ COSY NMR spectrum of <b>82</b> in $\text{CDCl}_3$	138
<b>Figure 3.123</b>	$^1\text{H}$ - $^1\text{H}$ COSY NMR spectrum of aromatic protons of <b>82</b>	138
<b>Figure 3.124</b>	$^1\text{H}$ - $^{13}\text{C}$ HMQC NMR spectrum of <b>82</b> in $\text{CDCl}_3$	139
<b>Figure 3.125</b>	Aromatic protons and carbons in $^1\text{H}$ - $^{13}\text{C}$ HMQC NMR spectrum of <b>82</b>	140
<b>Figure 3.126</b>	$^1\text{H}$ - $^{13}\text{C}$ HMBC NMR spectrum of <b>82</b> in $\text{CDCl}_3$	141
<b>Figure 3.127</b>	Aromatic protons and carbons in $^1\text{H}$ - $^{13}\text{C}$ HMBC NMR spectrum of <b>82</b>	141
<b>Figure 3.128</b>	The correlations observed in HMBC spectrum of <b>82</b>	142
<b>Figure 3.129</b>	The asymmetric unit of <b>82</b> . Displacement ellipsoids are drawn at the 30% probability level. Intramolecular interactions are shown as dashed lines	143
<b>Figure 3.130</b>	The chemical structure and the numbering scheme of <b>83</b>	147
<b>Figure 3.131</b>	FTIR spectrum of <b>83</b>	147
<b>Figure 3.132</b>	EIMS spectrum of <b>83</b>	149

<b>Figure 3.133</b>	HRMS spectrum of <b>83</b>	149
<b>Figure 3.134</b>	The proposed structures of the prominent peaks of <b>83</b>	150
<b>Figure 3.135</b>	$^1\text{H}$ NMR spectrum of <b>83</b> in $\text{CDCl}_3$	151
<b>Figure 3.136</b>	$^1\text{H}$ NMR spectrum of <b>83</b> in acetone- $d_6$	151
<b>Figure 3.137</b>	$^{13}\text{C}$ NMR spectrum of <b>83</b> in $\text{CDCl}_3$	153
<b>Figure 3.138</b>	$^{13}\text{C}$ NMR spectrum of <b>83</b> in acetone- $d_6$	153
<b>Figure 3.139</b>	$^1\text{H}$ - $^1\text{H}$ COSY NMR spectrum of <b>83</b> in $\text{CDCl}_3$	156
<b>Figure 3.140</b>	$^1\text{H}$ - $^1\text{H}$ COSY NMR spectrum of aromatic protons of <b>83</b> in $\text{CDCl}_3$	156
<b>Figure 3.141</b>	$^1\text{H}$ - $^1\text{H}$ COSY NMR spectrum of <b>83</b> in acetone- $d_6$	157
<b>Figure 3.142</b>	$^1\text{H}$ - $^1\text{H}$ COSY NMR spectrum of aromatic protons of <b>83</b> in acetone- $d_6$	157
<b>Figure 3.143</b>	The correlations observed in COSY spectrum of <b>83</b>	157
<b>Figure 3.144</b>	$^1\text{H}$ - $^{13}\text{C}$ HMQC NMR spectrum of <b>83</b> in $\text{CDCl}_3$	158
<b>Figure 3.145</b>	$^1\text{H}$ - $^{13}\text{C}$ HMQC NMR spectrum of <b>83</b> in acetone- $d_6$	158
<b>Figure 3.146</b>	$^1\text{H}$ - $^{13}\text{C}$ HMBC NMR spectrum of <b>83</b> in $\text{CDCl}_3$	159
<b>Figure 3.147</b>	$^1\text{H}$ - $^{13}\text{C}$ HMBC NMR spectrum of <b>83</b> in acetone- $d_6$	160
<b>Figure 3.148</b>	The correlations observed in HMBC spectrum of <b>83</b>	160
<b>Figure 3.149</b>	The crystal structure of <b>83</b> showing 50% probability displacement ellipsoids and the atomic numbering. The dashed line indicates intramolecular hydrogen bond	162
<b>Figure 3.150</b>	The crystal packing of <b>83</b> , viewed down the <i>b</i> axis. Intramolecular hydrogen bonds are shown as dashed lines	163
<b>Figure 3.151</b>	The chemical structure and the numbering scheme of <b>84</b>	164
<b>Figure 3.152</b>	The crystal structure of the bis-Schiff base <b>79</b>	166
<b>Figure 3.153</b>	FTIR spectrum of <b>84</b>	168
<b>Figure 3.154</b>	HRMS spectrum of <b>84</b>	168

<b>Figure 3.155</b>	The proposed structures of intense peaks of <b>84</b>	169
<b>Figure 3.156</b>	$^1\text{H}$ NMR spectrum of <b>84</b> in acetone- $d_6$	170
<b>Figure 3.157</b>	$^{13}\text{C}$ NMR spectrum of <b>84</b> in acetone- $d_6$	171
<b>Figure 3.158</b>	$^1\text{H}$ - $^1\text{H}$ COSY NMR spectrum of <b>84</b> in acetone- $d_6$	173
<b>Figure 3.159</b>	$^1\text{H}$ - $^1\text{H}$ COSY NMR spectrum of aromatic protons range of <b>84</b>	174
<b>Figure 3.160</b>	The correlations observed in COSY spectrum of <b>84</b>	174
<b>Figure 3.161</b>	$^1\text{H}$ - $^{13}\text{C}$ HMQC NMR spectrum of <b>84</b> in acetone- $d_6$	175
<b>Figure 3.162</b>	Aromatic protons and carbons in $^1\text{H}$ - $^{13}\text{C}$ HMQC NMR spectrum of <b>84</b>	175
<b>Figure 3.163</b>	$^1\text{H}$ - $^{13}\text{C}$ HMBC NMR spectrum of <b>84</b> in acetone- $d_6$	176
<b>Figure 3.164</b>	Aromatic protons and carbons in $^1\text{H}$ - $^{13}\text{C}$ HMBC NMR spectrum of <b>84</b>	176
<b>Figure 3.165</b>	The correlations observed in HMBC spectrum of <b>84</b>	177
<b>Figure 3.166</b>	The chemical structure of benzimidazole <b>89</b>	179
<b>Figure 3.167</b>	The chemical structure of benzimidazoles <b>73</b> , <b>74</b> and <b>98</b>	180
<b>Figure 3.168</b>	The structure of the evaluated benzimidazoles <b>77</b> , <b>78</b> , <b>83</b> and <b>84</b>	181
<b>Figure 3.169</b>	Dose response curve of the evaluated benzimidazole <b>84</b> with MCF-7 cancer cell	182
<b>Figure 3.170</b>	Dose response curve of the evaluated benzimidazole <b>77</b> with MCF-7 cancer cell	183
<b>Figure 3.171</b>	Dose response curve of the evaluated benzimidazole <b>78</b> with MCF-7 cancer cell	183
<b>Figure 3.172</b>	Dose response curve of the evaluated benzimidazole <b>83</b> with MCF-7 cancer cell	184
<b>Figure 3.173</b>	Dose response curve of the evaluated benzimidazole <b>78</b> with HCT-116 cancer cell	185
<b>Figure 3.174</b>	Dose response curve of the evaluated benzimidazole <b>77</b> with HCT-116 cancer cell	185

- Figure 3.175** Dose response curve of the evaluated benzimidazole **84** with HCT-116 cancer cell 186
- Figure 3.176** Dose response curve of the evaluated benzimidazole **83** with HCT-116 cancer cell 186

## LIST OF SCHEMES

	<i>Page</i>	
<b>Scheme 1.1</b>	First benzimidazole <b>6</b> , prepared by Hobrecker in 1872	4
<b>Scheme 1.2</b>	The Phillips-type to prepare the benzimidazole	8
<b>Scheme 1.3</b>	Preparation of benzimidazoles using the method of Wang <i>et al.</i>	8
<b>Scheme 1.4</b>	Benzimidazoles preparation in the presence of Na <sub>2</sub> S <sub>2</sub> O <sub>5</sub>	9
<b>Scheme 1.5</b>	Benzimidazoles preparation in the presence of NaHSO <sub>3</sub>	9
<b>Scheme 1.6</b>	Preparation of benzimidazoles using the method of Bahrami <i>et al.</i>	10
<b>Scheme 1.7</b>	The preparation of the benzimidazoles from MW irradiation	10
<b>Scheme 1.8</b>	Preparation of benzimidazoles using the method of Elderfield and Kreysa	11
<b>Scheme 1.9</b>	Benzimidazoles from $\beta$ -diketones	11
<b>Scheme 1.10</b>	Preparation of benzimidazoles using the method of Mamedov <i>et al.</i>	12
<b>Scheme 1.11</b>	Benzimidazoles from <i>o</i> -nitroarylamines	12
<b>Scheme 1.12</b>	Benzimidazoles from <i>o</i> -azidoarylamines	13
<b>Scheme 1.13</b>	Benzimidazoles from amidines	14
<b>Scheme 1.14</b>	Synthesize benzimidazoles by MW assay using the method of Lim <i>et al.</i>	14
<b>Scheme 1.15</b>	Synthesize benzimidazoles with Na <sub>2</sub> S <sub>2</sub> O <sub>5</sub> using the method of Ozden <i>et al.</i>	15
<b>Scheme 1.16</b>	Synthesize benzimidazoles with NaHSO <sub>3</sub> using the method of Kilcigil <i>et al.</i>	16
<b>Scheme 1.17</b>	Synthesize benzimidazoles with <i>p</i> -toluenesulfonic acid using the method of Rao <i>et al.</i>	16
<b>Scheme 1.18</b>	Benzimidazoles from MW irradiation by K-10 clay	17

<b>Scheme 1.19</b>	Synthesize benzimidazoles with 5-10% Pd(PPh <sub>3</sub> ) <sub>4</sub> using the method of Brain and Brunton	17
<b>Scheme 1.20</b>	Synthesize benzimidazoles using the method Vazquez <i>et al.</i>	18
<b>Scheme 1.21</b>	Synthesize benzimidazoles using the method of Goker <i>et al.</i> and Page <i>et al.</i>	19
<b>Scheme 1.22</b>	Synthesize Schiff bases and benzimidazoles using the method of Smith and Ho	19
<b>Scheme 1.23</b>	Synthesize Schiff bases and benzimidazoles using the method of Latif <i>et al.</i>	20
<b>Scheme 2.1</b>	Synthetic route towards compound <b>75</b>	30
<b>Scheme 2.2</b>	Synthetic route towards compounds <b>76</b> and <b>82</b>	31
<b>Scheme 2.3</b>	Synthetic route towards compounds <b>77</b> , <b>78</b> , <b>79</b> , <b>83</b> and <b>84</b>	33
<b>Scheme 2.4</b>	Synthetic route towards compounds <b>80</b> and <b>81</b>	34
<b>Scheme 3.1</b>	Synthetic route towards the preparation of compound <b>75</b>	39
<b>Scheme 3.2</b>	Synthesize Schiff base <b>85</b> using the method of Danheiser <i>et al.</i>	55
<b>Scheme 3.3</b>	Formation of compound <b>76</b>	55
<b>Scheme 3.4</b>	Preparation of compounds <b>77</b> , <b>78</b> and <b>79</b> from <b>76</b>	69
<b>Scheme 3.5</b>	Preparation of bis-Schiff base <b>80</b>	107
<b>Scheme 3.6</b>	Preparation of bis-Schiff base <b>81</b>	118
<b>Scheme 3.7</b>	Formation of benzeneamine <b>82</b>	131
<b>Scheme 3.8</b>	The tetrahedral mechanism to form <b>76</b> or <b>82</b>	132
<b>Scheme 3.9</b>	Formation of benzimidazoles <b>83</b> and <b>84</b>	145
<b>Scheme 3.10</b>	Formation of benzimidazoles <b>77</b> , <b>78</b> , <b>83</b> and <b>84</b> from amino benzeneamines <b>76</b> or <b>82</b>	146
<b>Scheme 3.11</b>	The proposed mechanism for the formation of bis-Schiff bases <b>79</b> or <b>86</b> from 2-amino benzeneamines <b>76</b> or <b>82</b>	165
<b>Scheme 3.12</b>	The proposed mechanism to form a tetrahedral intermediate <b>87</b> by the cyclization of the bis-Schiff bases <b>79</b> or <b>86</b>	166

**Scheme 3.13** The proposed mechanism to form the benzimidazoles **78** or **84** by 1,3-H sigmatropic rearrangement of a tetrahedral intermediate **87**

167

## LIST OF ABBREVIATIONS

- PPA = Polyphosphoric acid  
DMF = Dimethyl formamide  
DMA = *N,N*-Dimethyl acetamide  
AcOH = Acetic acid  
EtOH = Ethanol  
MeOH = Methanol  
CAN = Ceric ammonium nitrate  
DCM = Dichloromethane  
NMP = *N*-Methyl-2-pyrrolidone  
MW = Microwave irradiation  
Py. = Pyridine  
MS = Molecular sieves  
K-10 clay = montmorillonite  
HATU = *N,N,N,N*-Tetramethyl-*O*-(7-azabenzotriazole-1-yl) uranium hexafluoro-phosphate  
DIPEA = *N,N*-Diisopropylethylamine  
MTT = 3-(4,5-dimethylthiazol-2-yl)-2,5-diphenyltetrazolium bromide  
TBAI = Tetra-*n*-butylammonium iodide  
DMAP = *N,N*-4-Dimethyl aminopyridine  
PTC = Phase-transfer catalysts  
TBAB = Tetra-*n*-butylammonium bromide  
equiv. = equivalent  
Temp. = Temperature  
TLC = Thin layer chromatography  
 $R_f$  = Retention factor  
hr = hour  
min = minute  
mol = mole  
 $\Delta$  = heat  
rt = room temperature  
FTIR = Fourier-Transform Infrared

as = asymmetric

sy = symmetric

$\nu$  = stretching band

$\delta$  = bending band

EIMS = Electron-Ionization Mass Spectrum

HRMS = High-Resolution Mass Spectrum

NMR = Nuclear Magnetic Resonance

$\delta$  = chemical shift

ppm = part per million

TMS = tetramethylsilane

$J$  = coupling constant

Hz = Hertz

MHz = Megahertz

$s$  = singlet

$d$  = doublet

$t$  = triplet

$q$  = quartet

$m$  = multiplet

$dd$  = double doublet

$dq$  = double quartet

$td$  = triple doublet

$br$  = broad

APT = Attached Proton Test

DEPT = Distortionless Enhancement by Polarization Transfer

COSY = Correlation Spectroscopy

HMQC = Heteronuclear Multiple Quantum Coherence

HMBC = Heteronuclear Multiple Bond Coherence

$^{\circ}$  = degree

$\text{\AA}$  = angstrom unit ( $\equiv 10^{-10}$  m)

$\mu$  = absorption coefficient

$\theta$  = scattering angle

$\lambda$  = X-ray wavelength

$\sigma$  = standard error

$hkl$  = Miller indices

$F$  = structure factor

$F_o$  = observed structure factor

$I$  = reflection intensity

$R$  = conventional residual, calculated from  $F_o$ -data

$S$  = sign of a structure factor

$T$  = temperature

$V$  = volume

$w$  = weight of a structure factor

$wR$  = weighted residual, calculated from  $F_o$ -data

$wR_2$  = weighted residual, calculated from  $F_o^2$ -data

$Z$  = number of formula units per unit cell

MTT = 3-(4,5-dimethylthiazol-2-yl)-2,5-diphenyltetrazolium bromide

DMEM = Dulbecco's Modified Eagle Medium

PBS = Phosphate Buffer Saline

HIFCS = Heat inactivated fetal calf serum

OD = optical density

IC<sub>50</sub> = 50% inhibitory concentration

SD = Standard deviation

MCF-7 = Breast cancer cell line

HCT-116 = Colon cancer cell line

HT-29 = Colon cancer cell line

MDA-MB-231 = Human Breast cancer cell line

T-47D = Human Breast cancer cell line (Human breast ductal carcinoma cell)

HepG2 = Liver cancer cell line (Human hepatocellular carcinoma)

K562 = Leukaemia cell line (Human erythromyeloblastoid leukaemia cell line)

U937 = Leukaemia cell line (Human leukemic monocyte lymphoma cell line)

## LIST OF APPENDICES

	<i>Page</i>
<b>Appendix A-1</b> Crystal Data of <b>75</b>	207
<b>Appendix A-2</b> Crystal Data of <b>76</b>	208
<b>Appendix A-3</b> Crystal Data of <b>77</b>	209
<b>Appendix A-4</b> Crystal Data of <b>78A</b>	210
<b>Appendix A-5</b> Crystal Data of <b>78B</b>	211
<b>Appendix A-6</b> Crystal Data of <b>79</b>	212
<b>Appendix A-7</b> Crystal Data of <b>80</b>	213
<b>Appendix A-8</b> Crystal Data of <b>81</b>	214
<b>Appendix A-9</b> Crystal Data of <b>82</b>	215
<b>Appendix A-10</b> Crystal Data of <b>83</b>	216
<b>Appendix B-1</b> Tables of ELISA spectroscopy results for MCF-7 growth inhibition assay with the increase in <b>77</b> concentrations	217
<b>Appendix B-2</b> Tables of ELISA spectroscopy results for HCT-116 growth inhibition assay with the increase in <b>77</b> concentrations	218
<b>Appendix B-3</b> Tables of ELISA spectroscopy results for MCF-7 growth inhibition assay with the increase in <b>78</b> concentrations	219
<b>Appendix B-4</b> Tables of ELISA spectroscopy results for HCT-116 growth inhibition assay with the increase in <b>78</b> concentrations	220
<b>Appendix B-5</b> Tables of ELISA spectroscopy results for MCF-7 growth inhibition assay with the increase in <b>83</b> concentrations	221
<b>Appendix B-6</b> Tables of ELISA spectroscopy results for HCT-116 growth inhibition assay with the increase in <b>83</b> concentrations	222
<b>Appendix B-7</b> Tables of ELISA spectroscopy results for MCF-7 growth inhibition assay with the increase in <b>84</b> concentrations	223

**Appendix B-8** Tables of ELISA spectroscopy results for HCT-116 growth inhibition assay with the increase in **84** concentrations

224

# SINTESIS, PENCIRIAN DAN KAJIAN ANTI-PROLIFERASI TERBITAN BENZIMIDAZOL

## ABSTRAK

Empat jenis sebatian organik telah disintesis dan dicirikan. Sintesis sebatian ini melibatkan tindak balas pembenzilan, penambahan penyingkiran dan pensiklikan. Struktur sebatian yang disintesis dipastikan secara takat lebur, spektroskopi FTIR, HRMS, NMR 1D dan 2D dan kristalografi sinar-X. Sebatian jenis pertama adalah 2-benziloksi-3-metoksibenzaldehid **75**, yang telah disintesis dengan tindak balas *o*-vanilin dengan benzil bromida dalam aseton sebagai pelarut dan  $K_2CO_3$  sebagai bes dengan kehadiran tetra-*n*-butilammonium iodida (TBAI) sebagai mangkin. Sebatian jenis kedua yang dikaji adalah 2-amino-*N*-benzilidin benzenamina **76** dan **82**, yang disintesis dengan tindak balas *o*-fenilenadamina dengan *o*-vanilin atau **75** dalam diklorometana dalam keadaan sejuk. Kedua-dua eksperimen NMR  $^1H$ - $^1H$  COSY dan HMBC dijalankan untuk mengesahkan kedudukan jalur sebatian dalam  $CDCl_3$ ,  $CD_2Cl_2$  dan aseton- $d_6$ . Sebahagian kesan daripada gelang enam- dan lima- *illusory* terhasil daripada pembentukan intramolekul ikatan hidrogen antara N-H dalam gelang amino dan atom N dalam ikatan N=C-H dan O-H dengan atom N pada N=C-H pada **76** atau antara N-H dalam gelang amino dan atom N dalam ikatan N=C-H dan ikatan C-H metina pada **82** dengan atom oksigen dalam gelang benziloksi. Struktur kristal kedua **76** dan **82** disahkan dengan menggunakan analisis kristalografi sinar-X. Sebatian jenis ketiga yang dikaji adalah bes bis-Schiff **79**, **80** and **81**, yang dihasilkan dengan tindak balas antara *o*-vanillin dengan *o*-, *m*- dan *p*-fenilenadamina, masing-masing, oleh mekanisme tetrahedra atau mekanisme penambahan penyingkiran. Struktur kristal

bes bis-Schiff disahkan gelang enam- *illusory*, yang dihasilkan daripada pembentukan intramolekul ikatan hydrogen antara ikatan N=C-H dan kumpulan O-H pada gelang tritertukarganti yang disahkan dengan menggunakan analisis kristalografi sinar-X. Sebatian jenis keempat adalah benzimidazol **77**, **78**, **83** dan **84**, yang telah dihasilkan daripada amino benzenamina **76** and **82**, masing-masing, dalam media berakues atau berbes dengan mekanisme penambahan penyingkiran diikuti oleh mekanisme pensiklikan. Eksperimen NMR  $^1\text{H}$ ,  $^{13}\text{C}$ ,  $^1\text{H}$ - $^1\text{H}$  COSY, HMQC dan HMBC dijalankan untuk mengesahkan kedudukan jalur pada **77**, **78**, **83** dan **84**. Struktur kristal benzimidazol **77**, **78** dan **83** disahkan dengan menggunakan analisis kristalografi sinar-X. Semua benzimidazol telah dinilai terhadap titisan sel kanser payudara MCF-7 dan titisan sel kanser kolon HCT-116 menggunakan kaedah MTT. Keputusan benzimidazol **84** menunjukkan aktiviti sitotoksik yang tinggi terhadap titisan sel MCF-7 dengan  $\text{IC}_{50} = 8.86 \pm 1.10 \mu\text{g/mL}$ , dan aktiviti sitotoksik yang sederhana terhadap titisan sel HCT-116 dengan  $\text{IC}_{50} = 24.08 \pm 0.31 \mu\text{g/mL}$ . Manakala benzimidazol **78** menunjukkan  $\text{IC}_{50}$  rendah bernilai  $16.18 \pm 3.85 \mu\text{g/mL}$  terhadap titisan sel HCT-116. Kedua benzimidazol **77** dan **78** menunjukkan aktiviti sitotoksik yang sederhana terhadap titisan sel MCF-7, manakala benzimidazol **83** tidak menunjukkan sebarang aktiviti terhadap titisan sel MCF-7 dan HCT-116.

# SYNTHESIS, CHARACTERIZATION AND ANTI-PROLIFERATION STUDY OF SOME BENZIMIDAZOLE DERIVATIVES

## ABSTRACT

Four different types of compounds were successfully synthesized and characterized. The syntheses of these compounds involved benzylation, addition elimination and cyclization reactions. The structures of the synthesized compounds were confirmed by melting points, FTIR, HRMS, 1D and 2D NMR spectroscopy and X-ray crystallography. The first type of these compounds is 2-benzyloxy-3-methoxybenzaldehyde **75**, which was synthesized by the reaction of *o*-vanillin with benzyl bromide in acetone as the solvent and  $K_2CO_3$  as a base in the presence of tetra-*n*-butylammonium iodide (TBAI) as catalyst. The second type of the studied compounds is 2-amino-*N*-benzylidene benzeneamines **76** and **82**, which were synthesized from the reaction of *o*-phenylenediamine with *o*-vanillin or **75** in dichloromethane at cold conditions. Both  $^1H$ - $^1H$  COSY and HMBC NMR experiments were performed to further confirm the assigned peaks of compounds in  $CDCl_3$ ,  $CD_2Cl_2$  and acetone- $d_6$ . Some effect from those six- and five-membered illusory rings, which were formed from the intramolecular hydrogen bonding between N-H in the amino ring and the N atom in N=C-H bond and O-H with N atom of N=C-H of **76** or between N-H in the amino ring and the N atom in N=C-H bond and the bond of the methine C-H of **82** with oxygen atom in the benzyloxy ring. The crystal structures of both **76** and **82** confirmed the hydrogen bonds by using the X-ray crystallographic analysis. The third type of the studied compounds is bis-Schiff bases **79**, **80** and **81**, which are formed from the reaction between *o*-vanillin with *o*-, *m*- and *p*-phenylenediamines, respectively, by a tetrahedral mechanism or

addition/elimination mechanism. The crystal structures of those bis-Schiff bases confirmed six-membered illusory rings, which formed from the intramolecular hydrogen bonding between N=C-H bonds and O-H groups of the trisubstituted rings by using the X-ray crystallographic analysis. The fourth type of the studied compounds is benzimidazoles **77**, **78**, **83** and **84**, which are converted from amino benzeneamines **76** and **82**, respectively, in aqua or basic media by addition/elimination mechanism followed by cyclization. Those benzimidazoles have been evaluated against both breast cancer cell line MCF-7 and colon cancer cell line HCT-116 using MTT assay. The results of benzimidazole **84** showed high cytotoxic activity against MCF-7 cell lines with  $IC_{50} = 8.86 \pm 1.10 \mu\text{g/mL}$ , and moderate cytotoxic activity against HCT-116 cell lines with  $IC_{50} = 24.08 \pm 0.31 \mu\text{g/mL}$ . Benzimidazole **78** showed the lowest  $IC_{50}$  value at  $16.18 \pm 3.85 \mu\text{g/mL}$  against HCT-116 cell lines. Both benzimidazoles **77** and **78** showed moderate cytotoxic activity against MCF-7 cell lines, while benzimidazole **83** showed no cytotoxic effect with both MCF-7 and HCT-116 cell lines.

## CHAPTER ONE

## INTRODUCTION

## 1.1 Schiff bases

Schiff bases or imines are compounds formed from the condensation reaction between aldehydes or ketones and primary amines or amino acids in the presence of an acid catalyst (Figure 1.1). The product containing an azomethine, C=N linkage was discovered by Hugo Joseph Schiff (Layer, 1963; Cozzi, 2004). Many nomenclatures are used to describe the formation of Schiff bases, for example: aldimines, anils, benzanils and ketimines, derived from aldehydes, aniline, aromatic aldehydes and ketones, respectively (Layer, 1963; El-Bayoumi *et al.*, 1971*a,b*).

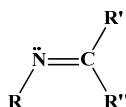


Figure 1.1: The general formula of Schiff base or imine.

These compounds are ranked among the most versatile synthetic organic intermediates, which are important for the synthesis of biologically important compounds. They are widely used as medical, pharmaceutical and industrial materials and were reported to show a variety of biological activities including as antifungal (Singh and Dash, 1988; More *et al.*, 2001), antibacterial (Baseer *et al.*, 2000; El-Masry *et al.*, 2000; Kabeer *et al.*, 2001) and anticancer (Kuz'min *et al.*, 2000; Desai *et al.*, 2001), among others. They also showed moderate activity against *Staphylococcus aureus* and *Bacillus subtilis* (Jarrahpour *et al.*, 2004).

They have also been used extensively in inorganic and coordination chemistry fields for the synthesis of new organometallic compounds. The imines formed from the reaction of the aldehydes and amines also proved to be the source of versatile compounds for many transition metals where they act as donor groups to bind the metal ions (Vigato and Tamburini, 2004). Besides that, Schiff bases are also used to produce new azo dyes (Jarrahpour and Zarei, 2004, Naeimi *et al.*, 2007). In another application, So *et al.* (2007) synthesized and characterized a series of Schiff base derivatives, which exhibited liquid crystal properties.

Bis-Schiff bases are produced from two equivalents of aldehyde or ketone with a diamine. The bases can be either symmetric or unsymmetric (asymmetric) structures, depending on the reacted aldehydes and diamines. Figure 1.2 shows examples of symmetric and unsymmetric bis-Schiff bases **1-4** (Lopez *et al.*, 1998*a,b*). Compounds **1** and **2** started off with symmetrical aromatic diamine ring, but the aldehyde rings are different. Compound **3** has symmetrical cyclic diamine ring with symmetrical aldehyde rings, while both diamine and aldehyde in compound **4** are unsymmetric.

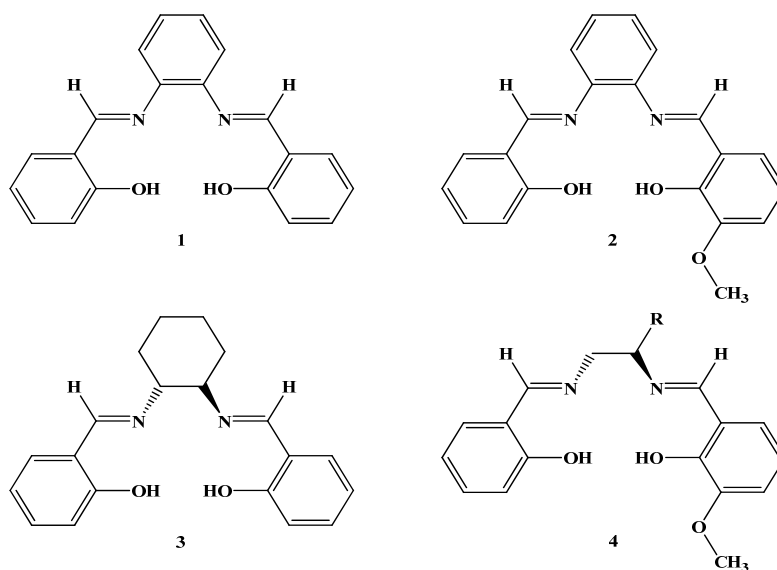


Figure 1.2: Some symmetrical and unsymmetrical bis-Schiff bases.

Both symmetrical and unsymmetrical bis-Schiff bases are interesting compounds particularly when they coordinate around the central metal ion to form transition metal ion complexes. For example, the symmetric bis-Schiff base complexes are normally used as macrocyclic models, while the unsymmetric complexes are used as irregular binding model with peptides (Atkins *et al.*, 1985). However, the unsymmetrical compounds are more advanced than their symmetrical counterparts in the explaining of the composition and geometry of metal ion binding sites in metalloproteins, leading to the enzymatic selectivity of the natural systems with synthetic materials (Bu *et al.*, 1997). Intercalation of other derivatives of symmetrical bis-Schiff bases with DNA by UV spectroscopy has also been studied (Parra *et al.*, 2007).

Various molecular structural studies on bis-Schiff bases and their complexes with different metal ions have been reported. Bis-Schiff bases and others were found to form suitable inner coordination sphere between tin atom with O and N atoms as quadridentate chelates (Teoh *et al.*, 1997). Ruthenium complexes of bis-Schiff bases derived from *o*-vanillin and salicylaldehyde however, showed dibasic tetradentate chelates (Viswanathamurthi *et al.*, 1998). An intramolecular hydrogen bond between the O and N atoms in Schiff bases is one of the important factors leading to the formation of metal complexes (Cohen *et al.*, 1964). Kabak *et al.* (2000) prepared the derivatives of bis-Schiff bases and studied their photochromic conformational properties. The intramolecular hydrogen bond causes a six-membered illusory ring to be formed between the O–H group at *ortho* position of the aldehydic moiety and N atom of the aminic moiety (Kawasaki *et al.*, 1999; Fukuda *et al.*, 2003); (Figure 1.3).

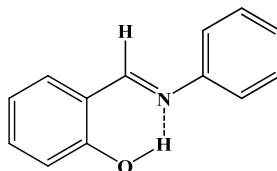


Figure 1.3: Intramolecular hydrogen bond.

## 1.2 Benzimidazoles

Benzimidazole (Figure 1.4) is a heterocyclic compound containing an imidazole ring fused at the 4,5-position with benzene ring. Hobrecker prepared the first benzimidazole in 1872 when he reduced 2-nitro-4-methylacetanilide, **5** to obtain the tautomers 2,5 (or 2,6)-dimethyl benzimidazole (**6**), (White, 1951; Hofmann, 1953); (Scheme 1.1).

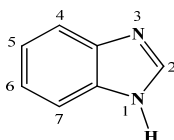
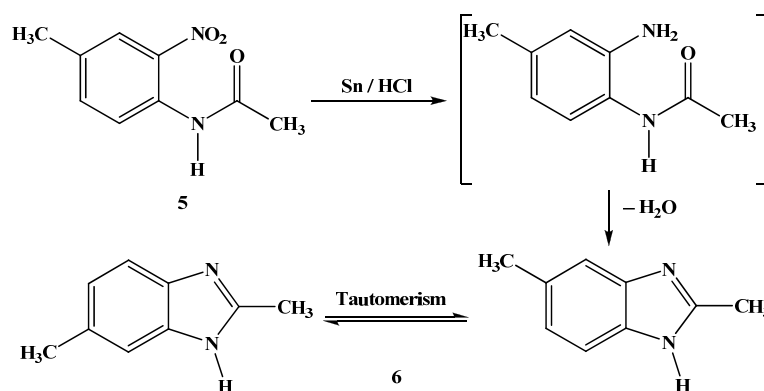


Figure 1.4: The benzimidazole ring.

Scheme 1.1: First benzimidazole **6**, prepared by Hobrecker in 1872 (White, 1951).

Since benzimidazoles have similar structures to purines, whose derivatives play important roles in biological systems; substituted benzimidazoles also showed interesting biological activities. For example, the ring of the benzimidazoles is found

as an integral part in the chemical structure of vitamin B<sub>12</sub>, **7** (Bonnett, 1963; Preston, 1974); (Figure 1.5).

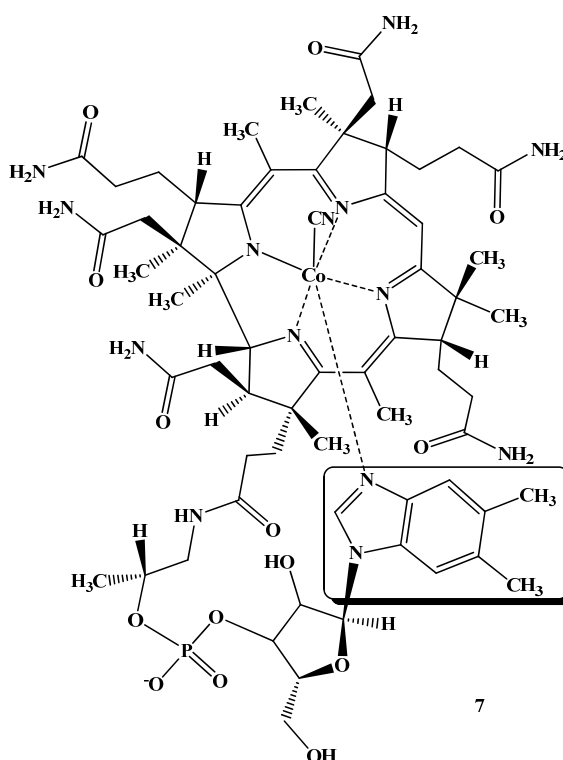


Figure 1.5: The benzimidazole ring in the chemical structure of vitamin B<sub>12</sub>, **7**.

Many benzimidazoles are pharmaceutical agents and used widely in biological system applications (Townsend and Revankav; 1970; Trivedi *et al.*, 2006). Some derivatives of benzimidazoles were reported and used as antiviral agents (**8-9**, Gudmundsson *et al.*, 2000; Cheng *et al.*, 2005), topoisomerase I inhibitors (**10-11**, Kim *et al.*, 1996, 1997; Rangarajan *et al.*, 2000; Mekapati and Hansch, 2001) and as antiproliferative agent (**12**, Hong *et al.*, 2004), (Figure 1.6).

Some of 4,5,6,7-tetrahalo-1*H*-benzimidazoles (**13**) were synthesised and showed antiprotozoal activity against *Acanthamoeba castellanii* (Kopanska *et al.*, 2004), antimycobacterial activity against *Mycobacterium* strains (**14**, Kazimierczuk *et al.*, 2005). In other studies, they can also act as antibacterial agents (**15-16**, Ozden

*et al.*, 2005; Nezhad *et al.*, 2005), and showed anthelmintic activity against *Trichinella spiralis* (Mavrova *et al.*, 2005), anti-inflammatory and analgesic activities (17, Sondhi *et al.*, 2006) and as inhibitors for hepatitis B (Li *et al.*, 2006) and C viruses (18, Beaulieu *et al.*, 2004). Some benzimidazoles were also tested as anti-HIV (19, Roth *et al.*, 1997; Smith *et al.*, 2003) and anticancer agents (20-21, Craig *et al.*, 1999; Rida *et al.*, 2006).

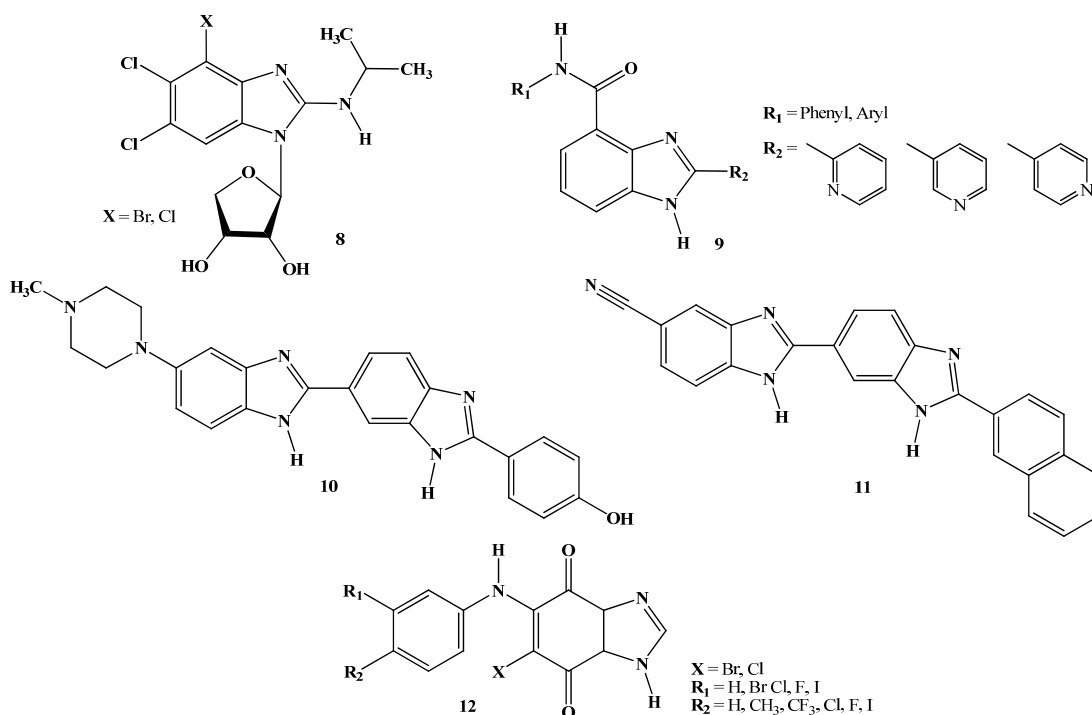


Figure 1.6: The chemical structures of some benzimidazole derivatives evaluated medicinally.

Recent publication also reported the use of phenolic and anisolic benzimidazole derivatives in vasodilator and antihypertensive studies (Soto *et al.*, 2006), while other alkyloxyaryl benzimidazole derivatives have been tested for the spasmolytic activity (Vazquez *et al.*, 2006). Figure 1.7 shows the chemical structures of many useful benzimidazole derivatives evaluated for biological activities.

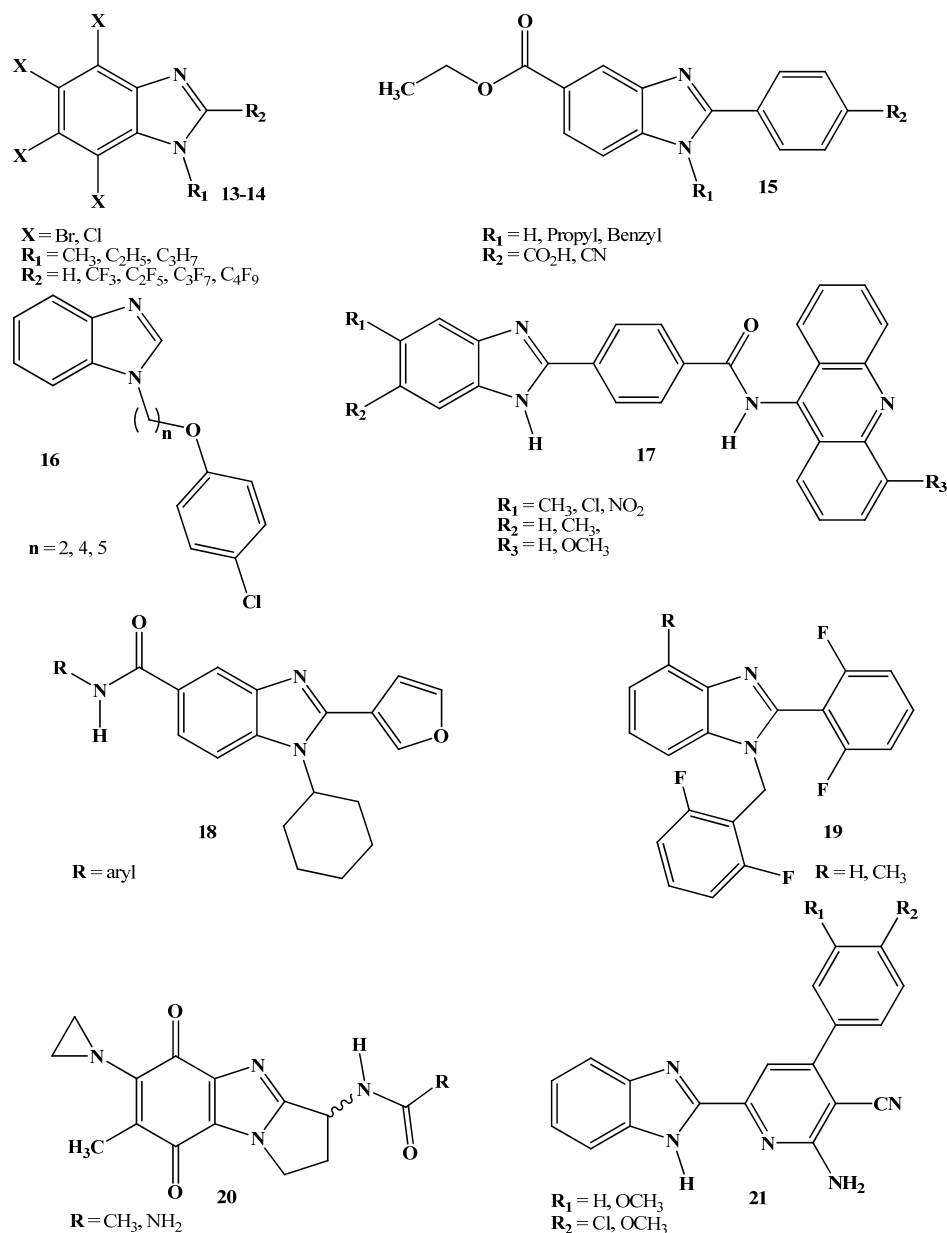


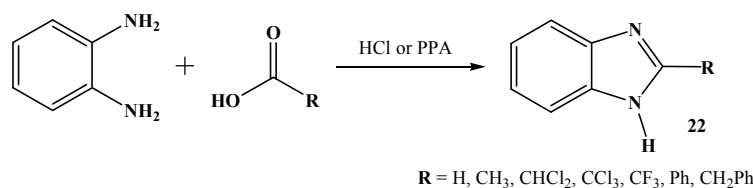
Figure 1.7: Some benzimidazole derivatives evaluated for biological activity.

The preparation of benzimidazole derivatives is well established. Monosubstitution occurs mainly at position 2, while the disubstitution at positions 1 and 2.

## 1.2.1 Substitution at position 2

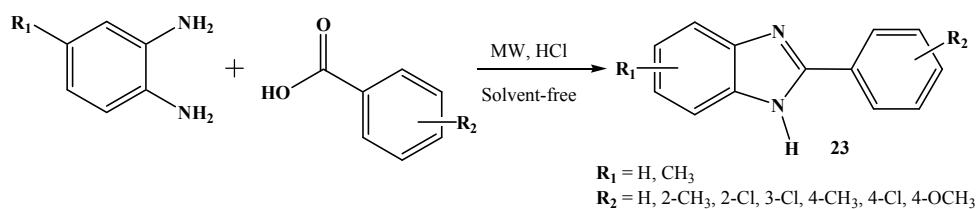
### 1.2.1.1 Reaction of *o*-arylene diamines with carboxylic acids

The Phillips-type method follows the reaction of *o*-arylene diamines with carboxylic acids or their derivatives using hydrochloric acid or polyphosphoric acid (PPA) as a catalyst to produce the respective benzimidazoles **22**, (Scheme 1.2). The benzimidazoles can also be produced from both reactants at 18 °C for 120 hr at pH 0.5 (Haley and Maitland, 1951).



Scheme 1.2: The Phillips-type to prepare the benzimidazole.

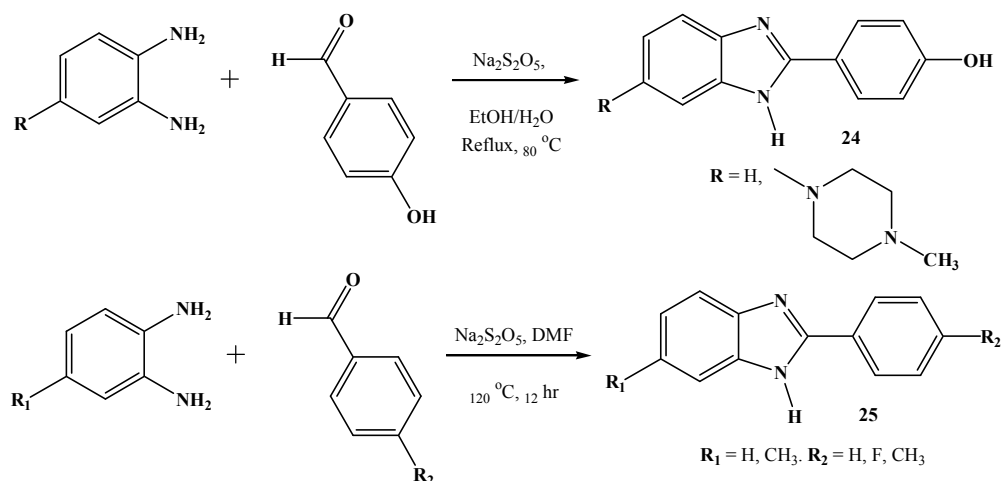
In solvent-free conditions with 7-10 mol % 8N HCl as a catalyst, a mixture of *o*-arylene diamines with carboxylic acids or their derivatives reacted in a domestic microwave oven at 600 W for 10 min to produce benzimidazoles **23** (Wang *et al.*, 2007; Scheme 1.3).



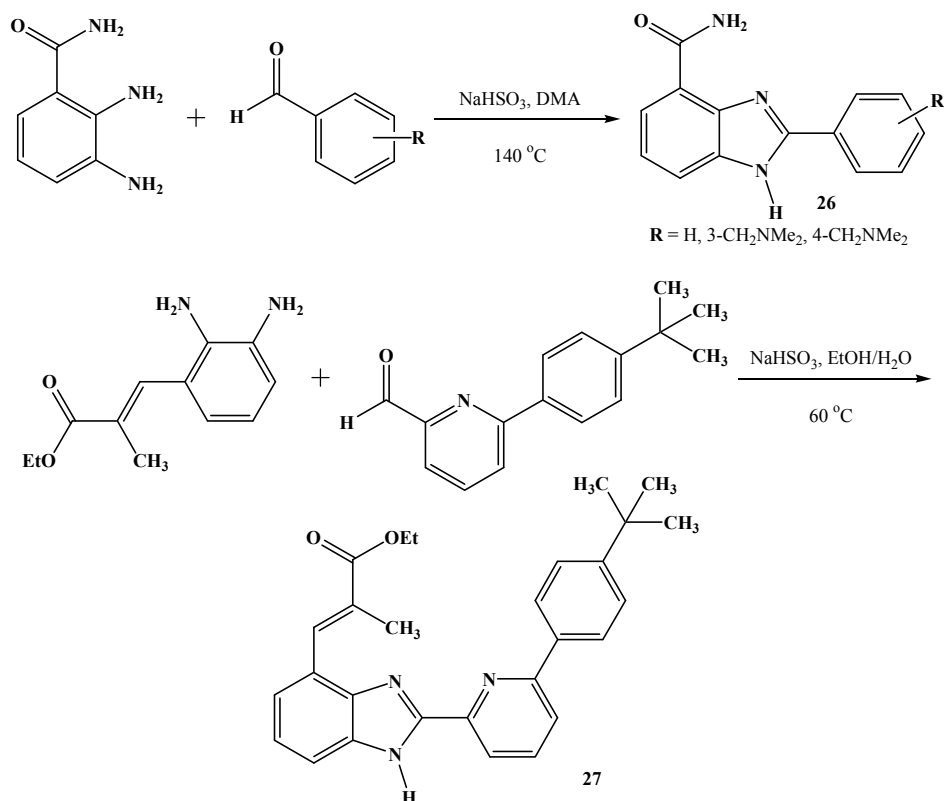
Scheme 1.3: Preparation of benzimidazoles using the method of Wang *et al.*

### 1.2.1.2 Reaction of *o*-arylene diamines with aldehydes

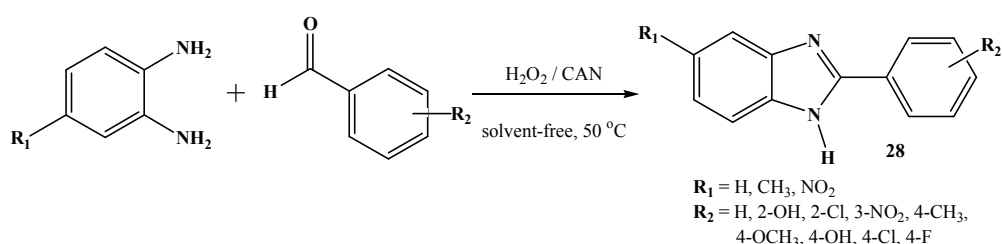
Kamal *et al.* (2004) prepared benzimidazoles **24** by reacting *o*-arylene diamines with 4-hydroxybenzaldehydes in ethanolic solution under reflux in the presence of Na<sub>2</sub>S<sub>2</sub>O<sub>5</sub> as oxidizing reagent, while Falco *et al.* (2006) used the same oxidizing reagent to prepared benzimidazoles **25** in dimethylformamide (DMF) under reflux for 12 hr, (Scheme 1.4).

Scheme 1.4: Benzimidazoles preparation in the presence of  $\text{Na}_2\text{S}_2\text{O}_5$ .

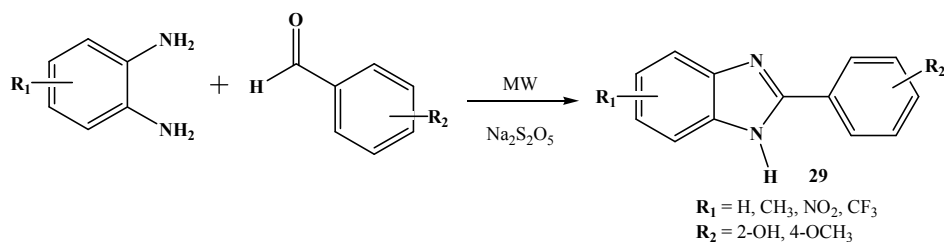
Other benzimidazole derivatives **26-27** were yielded by refluxing *o*-arylene diamines with benzaldehydes in the presence of  $\text{NaHSO}_3$  as oxidizing reagent at 140 °C in *N,N*-dimethylacetamide (DMA) or in EtOH/H<sub>2</sub>O at 60 °C, respectively (White *et al.*, 2004; Safonov *et al.*, 2006); (Scheme 1.5).

Scheme 1.5: Benzimidazoles preparation in the presence of  $\text{NaHSO}_3$ .

Meanwhile, Bahrami *et al.* (2008) described a new convenient method for the synthesis of benzimidazole derivatives **28** by the reaction of substituted *o*-arylene diamines with aromatic aldehydes in the presence of ceric ammonium nitrate (CAN) as a catalytic redox reagent and H<sub>2</sub>O<sub>2</sub> in free solvent for 10-70 min at 50 °C; (Scheme 1.6). Under microwave irradiation at 1000 W, the reaction between aldehydes and *o*-arylene diamines afforded the benzimidazole derivatives **29** (Soto *et al.*, 2006; Scheme 1.7).



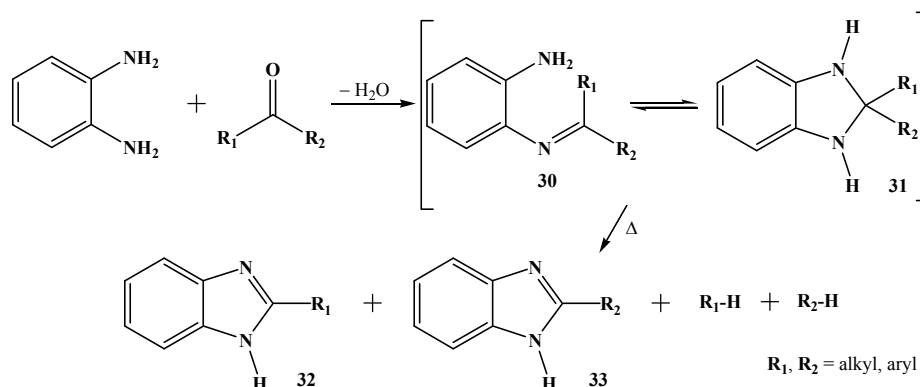
Scheme 1.6: Preparation of benzimidazoles using the method of Bahrami *et al.*



Scheme 1.7: The preparation of the benzimidazoles from MW irradiation.

### 1.2.1.3 Reaction of *o*-arylene diamines with ketones

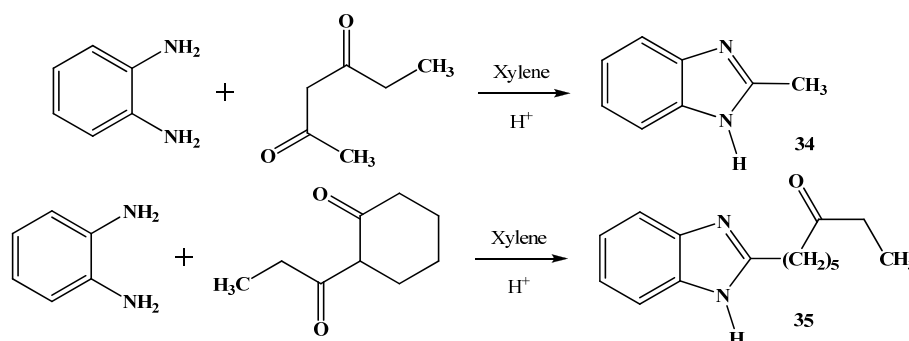
2-Disubstituted benzimidazoline **31** was formed from the reaction between *o*-arylene diamines and ketones by elimination of water, which decomposed under heat to produce 2-substituted benzimidazoles, **32-33** and hydrocarbons (Elderfield and Kreysa, 1948); (Scheme 1.8). The intermediate **31** was isolated with its tautomer **30** (Elderfield and Meyer, 1954*a,b*).



Scheme 1.8: Preparation of benzimidazoles using the method of Elderfield and Kreysa.

#### 1.2.1.4 Benzimidazole derivatives from $\beta$ -diketone

Benzimidazole derivatives can also be synthesized from  $\beta$ -diketone. This was described by Rossi *et al.* (1960) when *o*-phenylenediamine was heated with  $\beta$ -diketone derivatives in xylene with acidic media to furnish good yields of **34-35** (Scheme 1.9).

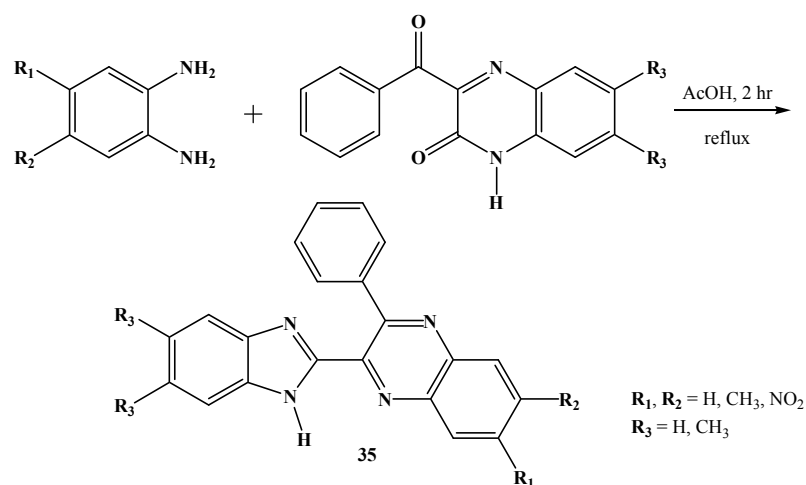


Scheme 1.9: Benzimidazoles from  $\beta$ -diketones.

#### 1.2.1.5 Benzimidazoles from the reaction of *o*-arylene diamines with quinoxalin-2-one derivatives

Novel benzimidazoles were obtained from the reaction between *o*-arylene diamines and quinoxalin-2-one derivatives under reflux in acetic acid for 2 hr to afford 2-benzimidazolylquinoxaline derivatives, **35**. Good yield of **35** was obtained,

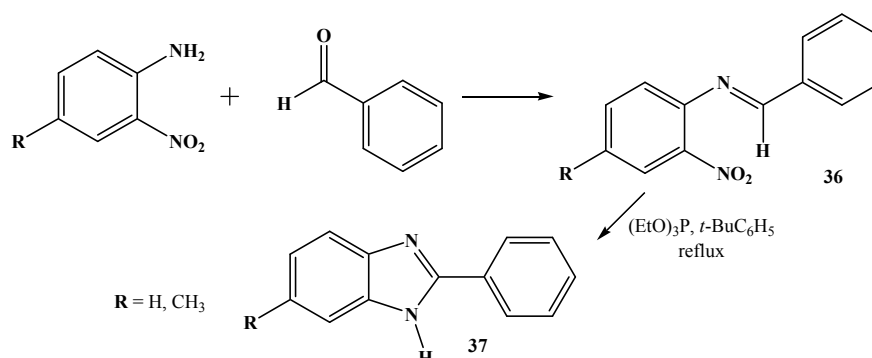
which depends on the position of R in *o*-phenylenediamine (Mamedov *et al.*, 2008); (Scheme 1.10).



Scheme 1.10: Preparation of benzimidazoles using the method of Mamedov *et al.*

### 1.2.1.6 Benzimidazoles from *o*-nitroarylamines

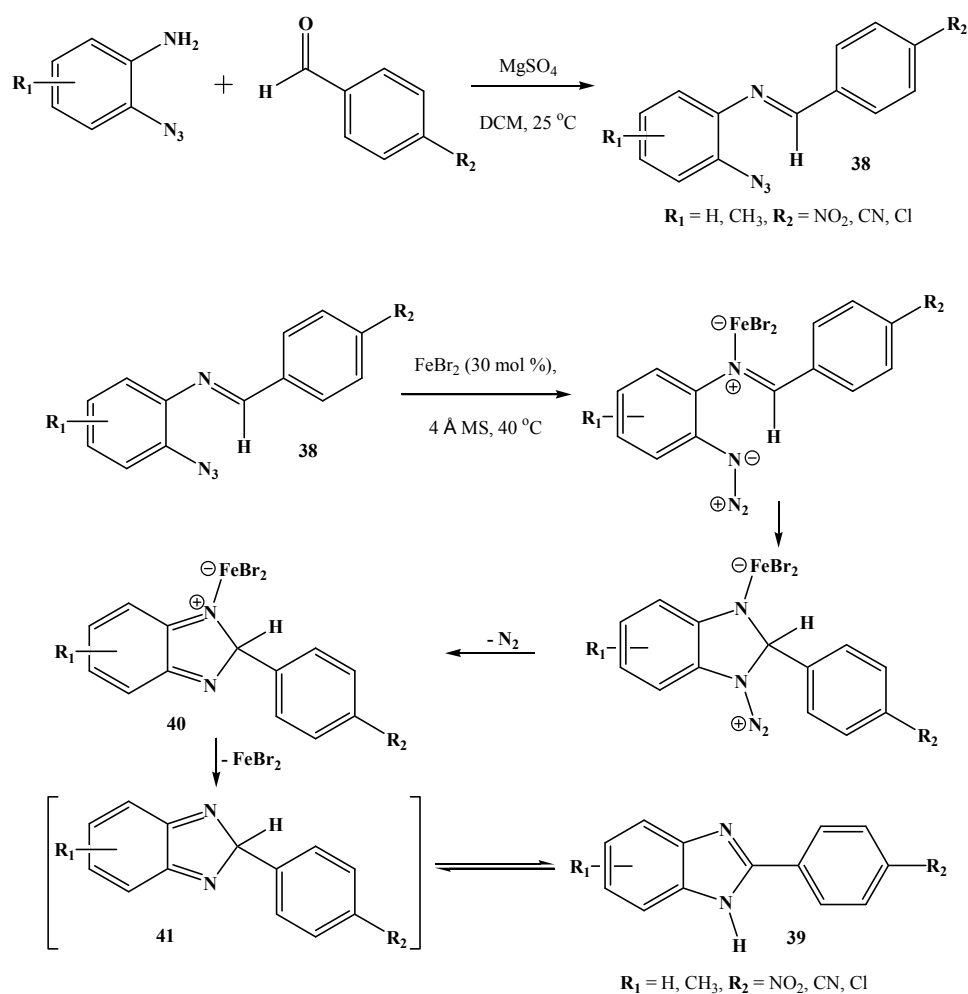
The reaction between *o*-nitroarylamines and aldehydes forms *N*-benzylidene-2-nitroaniline derivatives **36**, which was converted to 2-substituted benzimidazole derivatives **37** by the reductive cyclization using trialkyl phosphite (Smith and Suschitzky, 1961; Scheme 1.11). The trialkyl phosphite which acts as a reducing agent reduced the nitro group, followed by intramolecular cyclization process to produce **37** (Grimmett, 1997).



Scheme 1.11: Benzimidazoles from *o*-nitroarylamines.

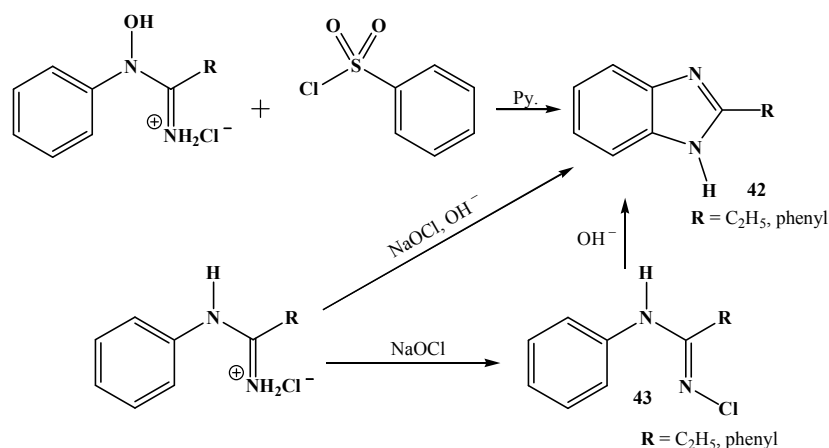
1.2.1.7 Benzimidazoles from *o*-azidoanilines

Thermolysis method is used to react *o*-azidoarylamines with aldehydes to produce good yields of *N*-benzylidene-2-azidoaniline derivatives, **38**, which were converted to 2-substituted benzimidazole derivatives, **39** (Krbecek and Takimoto, 1964; Hall and Kamm, 1965). Recently, Shen and Driver (2008) synthesized benzimidazoles from *o*-azidoanilines in two steps; using MgSO<sub>4</sub> in dichloromethane (DCM) at room temperature for 36 hr, followed by the addition of 30 mol % FeBr<sub>2</sub> as a catalyst with 4 Å molecular sieves in DCM at 40 °C for 12 hr (Scheme 1.12). Ferrous bromide, a Lewis acid was coordinated to the imine nitrogen to increase the electronegativity of **38**, followed by the reduction to generate **40**, which dissociated from iron catalyst to produce **41**. The tautomerisation of **41** gave **39**.

Scheme 1.12: Benzimidazoles from *o*-azidoarylamines.

### 1.2.1.8 Benzimidazoles from amidines

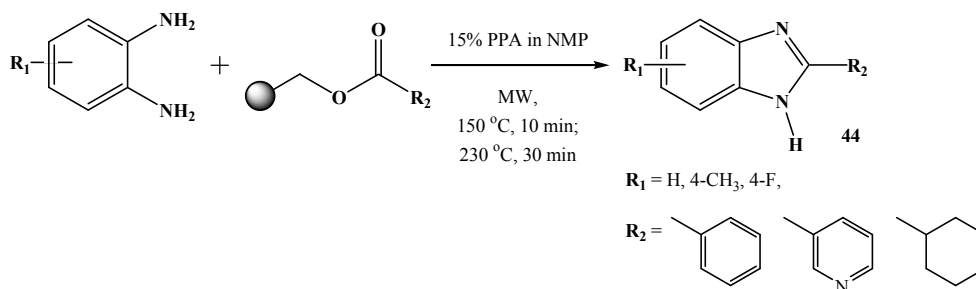
There are two ways of synthesizing benzimidazole derivatives **42** from amidines; i) by the reaction of *N*-arylamidines with benzenesulfonyl chloride in a base under anhydrous conditions (Preston, 1974), ii) by the oxidation of the amidines using sodium hypochlorite in basic media *via N*-chloroamidines **43** (Grenda *et al.*, 1965); (Scheme 1.13).



Scheme 1.13: Benzimidazoles from amidines.

### 1.2.1.9 Benzimidazoles from resin-bound esters

Lim *et al.* (2008) prepared 2-substituted benzimidazoles **44** from the condensation process between *o*-arylene diamines and resin-bound esters under microwave irradiation condition in the presence of PPA and *N*-Methyl-2-pyrrolidone (NMP) at 150 °C for 10 min and then 230 °C for 30 min to give an excellent yield (Scheme 1.14).

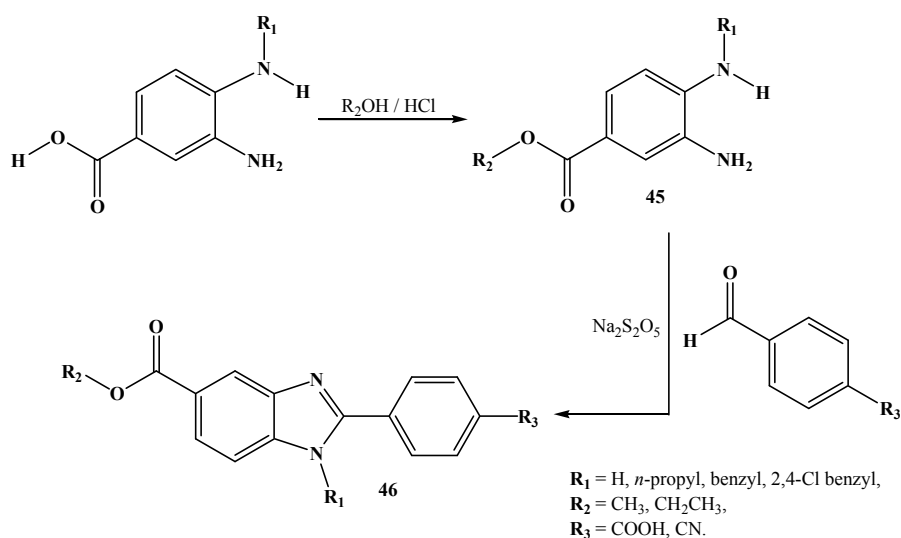


Scheme 1.14: Synthesize benzimidazoles by MW assay using the method of Lim *et al.*

## 1.2.2 1,2-Disubstitution of benzimidazoles

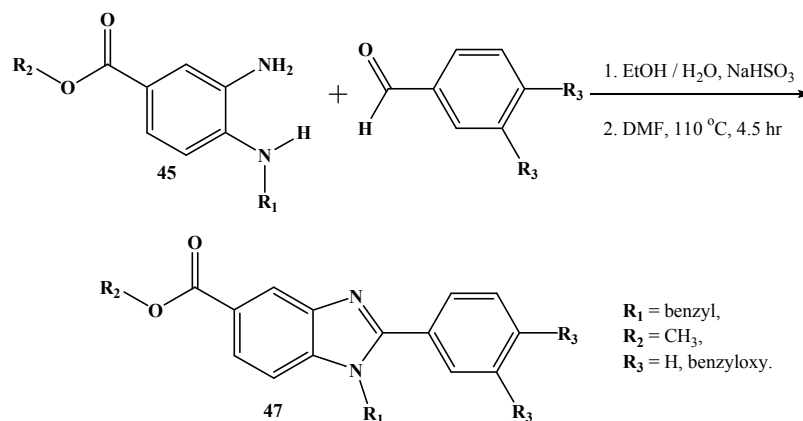
### 1.2.2.1 Benzimidazoles from *o*-arylene amines

The protection of one of the amino groups in *o*-arylene amines produced a derivative of *N*-substituted *o*-arylenediamine **45**. A cyclization of **45** with the second molecule of aldehyde derivatives in the presence of  $\text{Na}_2\text{S}_2\text{O}_5$  as an oxidizing reagent produced the benzimidazole derivative **46** (Ozden *et al.*, 2005); (Scheme 1.15).

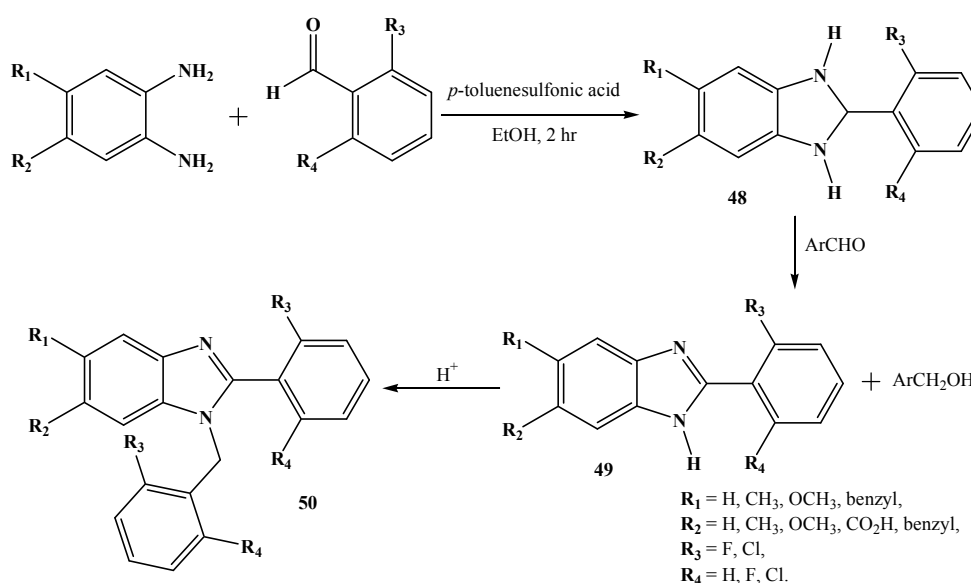


Scheme 1.15: Synthesize benzimidazoles with  $\text{Na}_2\text{S}_2\text{O}_5$  using the method of Ozden *et al.*

Kilcigil *et al.* (1999, 2003) used oxidative condition by adding  $\text{NaHSO}_3$  in DMF at  $110^\circ\text{C}$  for 4.5 hr to prepare the benzimidazoles **47** from **45** (Scheme 1.16). Both **46** and **47** were evaluated as having antimicrobial activity against for *Candida albicans*. The reaction of two moles of aldehyde derivatives with one mole of *o*-arylene amine in the presence of a catalytic amount of *p*-toluenesulfonic acid produces 2-arylbenzimidazoline **48**, which is converted to alcohols and 2-arylbenzimidazole derivative **49** by redox process. Benzimidazole derivative **50** is generated when **49** is heated in ethanolic solution. The product was then tested as an anti-HIV agent (Rao *et al.*, 2002); (Scheme 1.17).

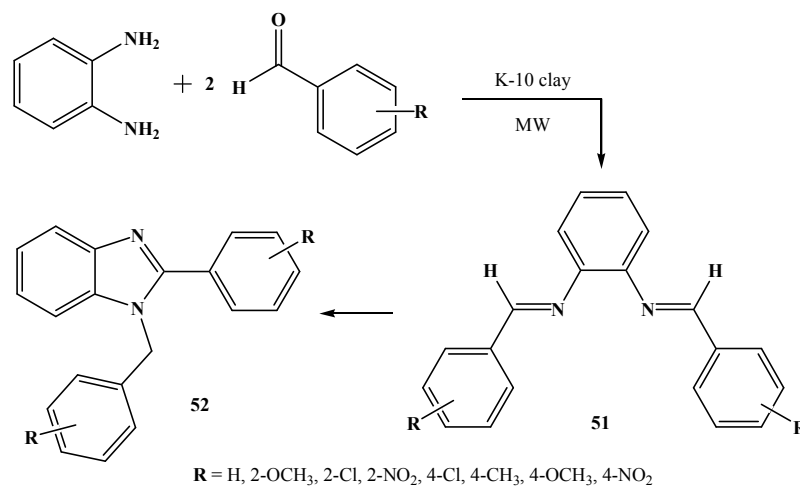


Scheme 1.16: Synthesize benzimidazoles with  $\text{NaHSO}_3$  using the method of Kilcigil *et al.*



Scheme 1.17: Synthesize benzimidazoles with *p*-toluenesulfonic acid using the method of Rao *et al.*

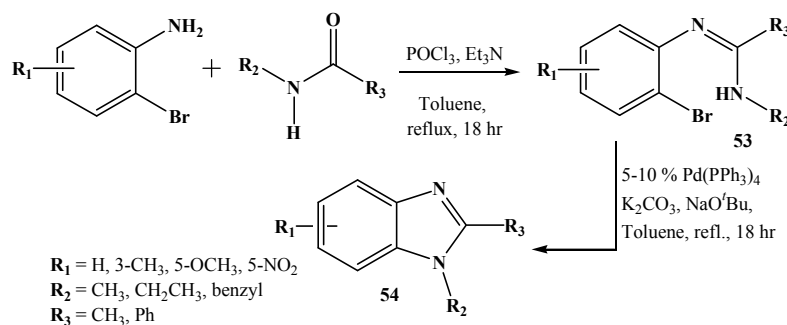
In another method, Perumal *et al.* (2006) reacted two moles of various aldehydes with *o*-phenylenediamines in the presence of montmorillonite K-10 under microwave irradiation and in the absence of solvent to produce bis-Schiff bases **51**, which is cyclized thermally to benzimidazole derivatives **52**; (Scheme 1.18).



Scheme 1.18: Benzimidazoles from MW irradiation by K-10 clay.

### 1.2.2.2 Benzimidazoles from *o*-haloarylamines

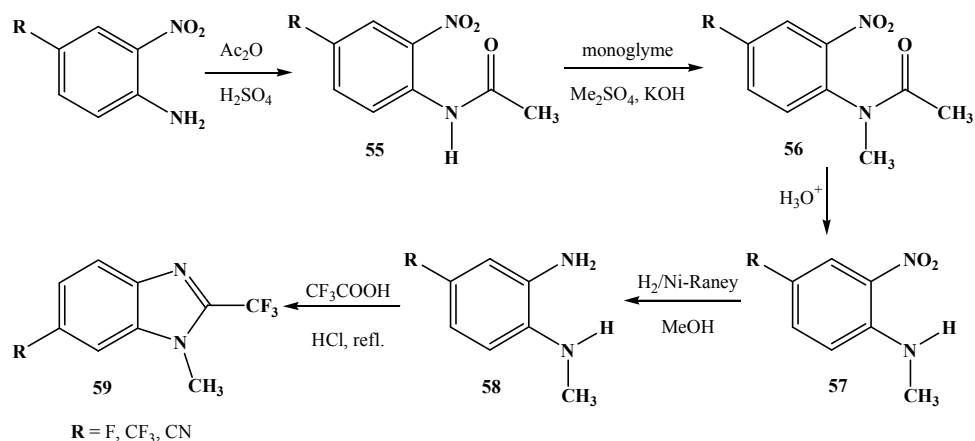
The amidation of *o*-haloarylamines to **53** occurred by heating a mixture of 2-bromoanilines with the amides in the presence of POCl<sub>3</sub> in toluene. It was then treated with 5–10% Pd(PPh<sub>3</sub>)<sub>4</sub> catalyst mixed with NaO<sup>t</sup>Bu and K<sub>2</sub>CO<sub>3</sub> in toluene for 18 hr under reflux to yield benzimidazole **54** (Brain and Brunton, 2002); (Scheme 1.19).

Scheme 1.19: Synthesize benzimidazoles with 5-10% Pd(PPh<sub>3</sub>)<sub>4</sub> using the method of Brain and Brunton.

### 1.2.2.3 Benzimidazoles from *o*-nitroarylamines

The acetylation of *o*-nitroarylamines with Ac<sub>2</sub>O using H<sub>2</sub>SO<sub>4</sub> as catalyst produced the acetanilide **55**, which was treated with Me<sub>2</sub>SO<sub>4</sub> and KOH to form *N*-methylated acetamide **56**. Addition of H<sub>2</sub>SO<sub>4</sub>, hydrolyzed **56** to *N*-methyl-2-

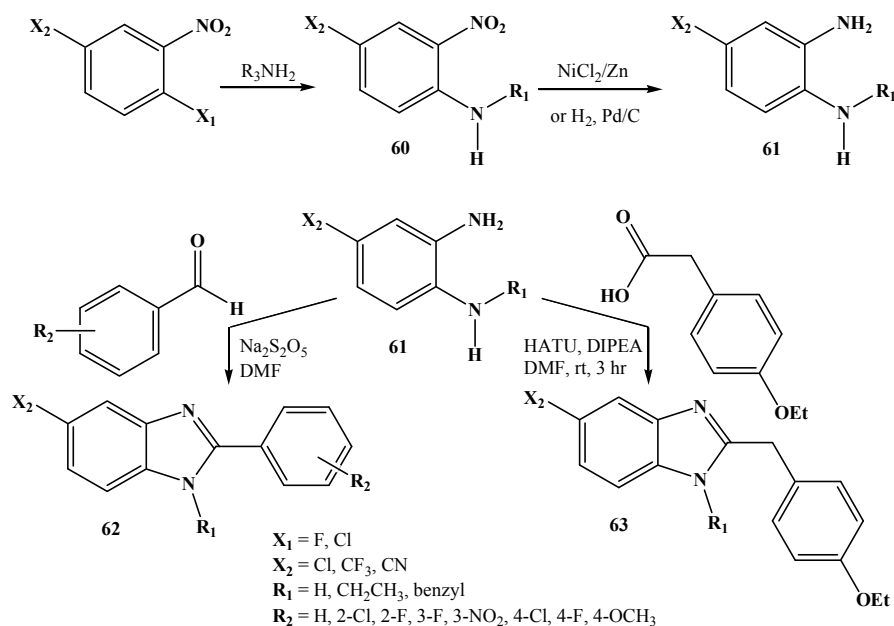
nitroaniline, **57**, which was reduced by  $H_2$  and Ni-Raney to afford *o*-phenylenediamine **58**. The benzimidazole **59** was produced by refluxing **58** with  $CF_3COOH$ . Compound **59** showed antiparasitic activity against *Giardia intestinalis*, *Trichomonas vaginalis* and *Plasmodium falciparum* (Vazquez *et al.*, 2006); (Scheme 1.20).



Scheme 1.20: Synthesize benzimidazoles using the method of Vazquez *et al.*

#### 1.2.2.4 Benzimidazoles from *o*-halonitrobenzenes

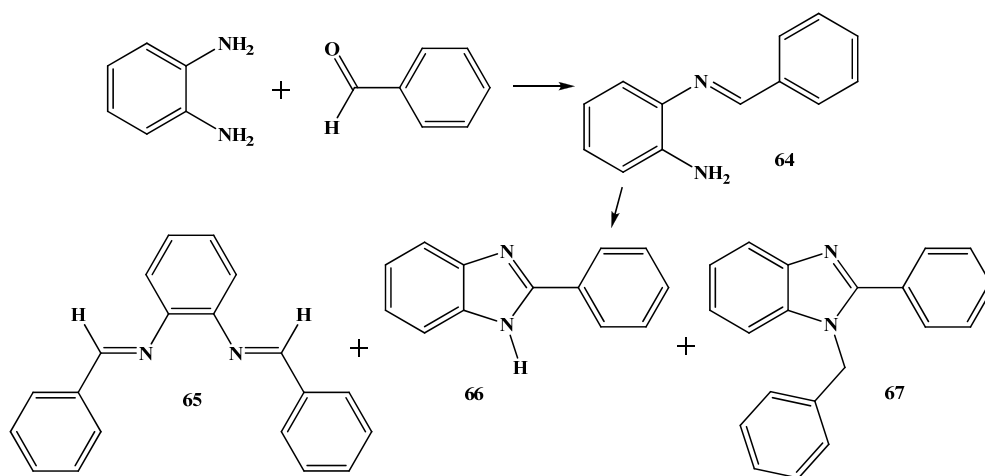
Many researchers have reported the methods to synthesize benzimidazoles **62** and **63** starting from *o*-halonitrobenzene derivatives, which was then aminated to produce *o*-nitroarylamine **60**. The reduction of **60** with  $NiCl_2/Zn$  or with  $H_2$  and Pd/C afforded *o*-phenylenediamine derivative **61**. The cyclization of **61** with corresponding benzaldehydes in the presence of  $Cu(AcO)_2/H_2S$ , or in the presence of  $Na_2S_2O_5$  in DMF gave benzimidazoles **62** and **63** (Goker *et al.*, 1998, 2002). However, using carboxylic acid derivatives in the presence of *N,N,N',N'*-tetramethyl-*O*-(7-azabenzotriazole-1-yl) uranium hexafluorophosphate (HATU) as a coupling reagent and a base *N,N*-diisopropylethylamine (DIPEA) or Hunig's base in DMF under acidic condition, afforded benzimidazole **63** (Page *et al.*, 2008; Scheme 1.21).



Scheme 1.21: Synthesize benzimidazoles using the method of Goker *et al.* and Page *et al.*

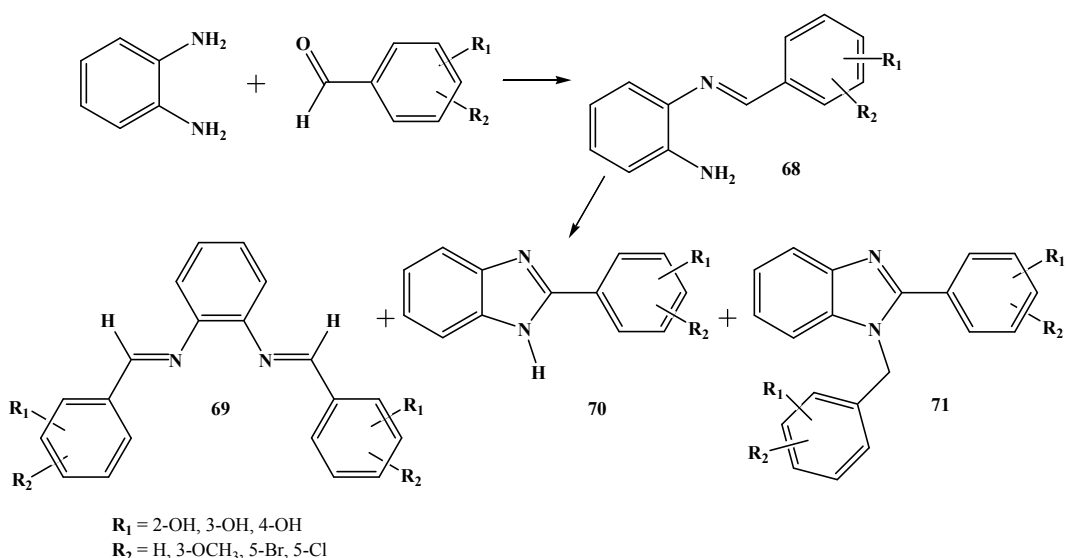
### 1.2.3 Synthesis leading to the formation of both Schiff base and benzimidazoles

Smith and Ho (1971) described the reaction of *o*-phenylenediamine with benzaldehyde by oxidative process in their preparation of 2-amino-*N*-benzylidene aniline, **64**, *N,N'*-dibenzal-*o*-phenylenediamine, **65**, 2-phenylbenzimidazole, **66** and 1-benzyl-2-phenylbenzimidazole, **67** (Scheme 1.22).



Scheme 1.22: Synthesize Schiff bases and benzimidazoles using the method of Smith and Ho.

Latif *et al.* (1983) reported in great detail the reaction of some phenolic aldehydes with *o*-phenylenediamine in boiling ethanolic solution, and they isolated the intermediates, **68**. Bis-Schiff bases **69** and benzimidazoles **70-71** produced from the reaction in most cases depended largely on the substituents in the phenyl ring of the aldehyde and the solvent used in the reflux process (Scheme 1.23).



Scheme 1.23: Synthesize Schiff bases and benzimidazoles using the method of Latif *et al.*

Both methods resulted in the formation of intermediates **64** and **68** from the reaction of one molecule of aldehyde derivatives with *o*-phenylenediamine under low temperature. However, the bis-Schiff bases **65** and **69**, including the benzimidazoles **66**, **67**, **70** and **71** were formed when **64** or **68** reacted with the second molecule of aldehyde derivative under reflux with nitrobenzene or 1-butanol.

Benzimidazole **73** is an analogue of the natural products **72**, which were synthesized from benzoic acid in multiple steps by Kumar *et al.* (2002) which produced moderate yields. Other benzimidazole derivative **74** was also prepared from the condensation of benzoic acid with *o*-phenylenediamine derivative. The natural products **72** were isolated from acetone extract of *Streptomyces* sp. 517-02

(Shibata *et al.*, 1993; Ueki *et al.*, 1993; Ueki and Taniguchi, 1997) and from *Streptomyces* sp. AJ956 (Sato *et al.*, 2001, Figure 1.8). Both **73** and **74** lacked of cytotoxicity activity against a range of cancer cell lines (Kumar *et al.*, 2002; Huang *et al.*, 2006).

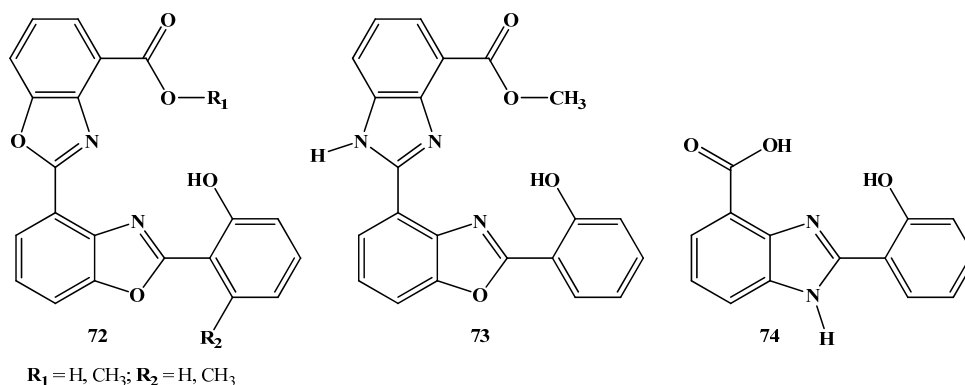
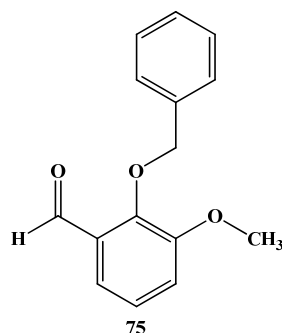
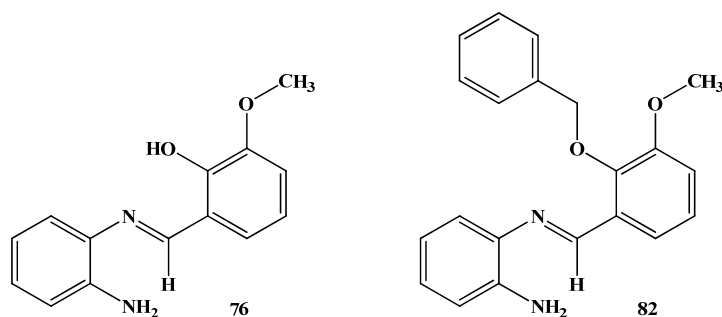


Figure 1.8: Benzimidazole derivatives evaluated against cancer cell lines.

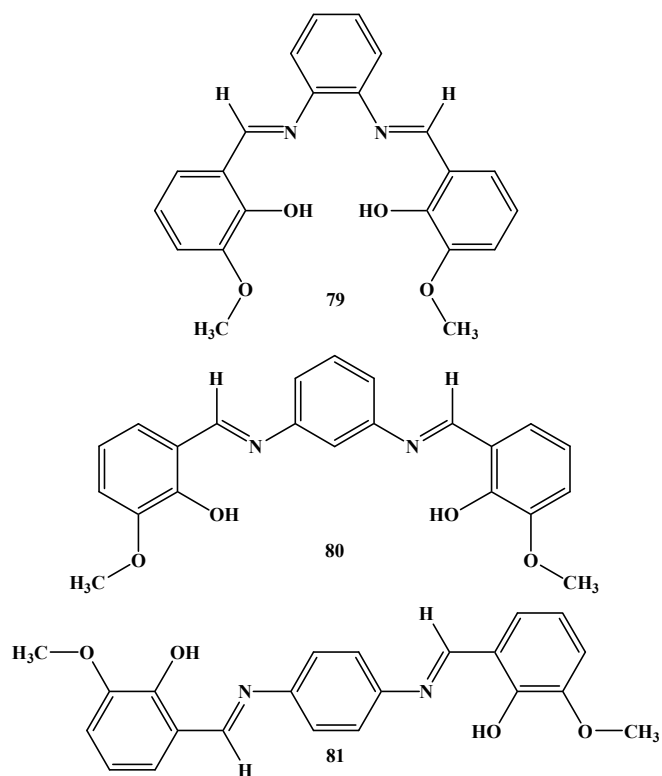
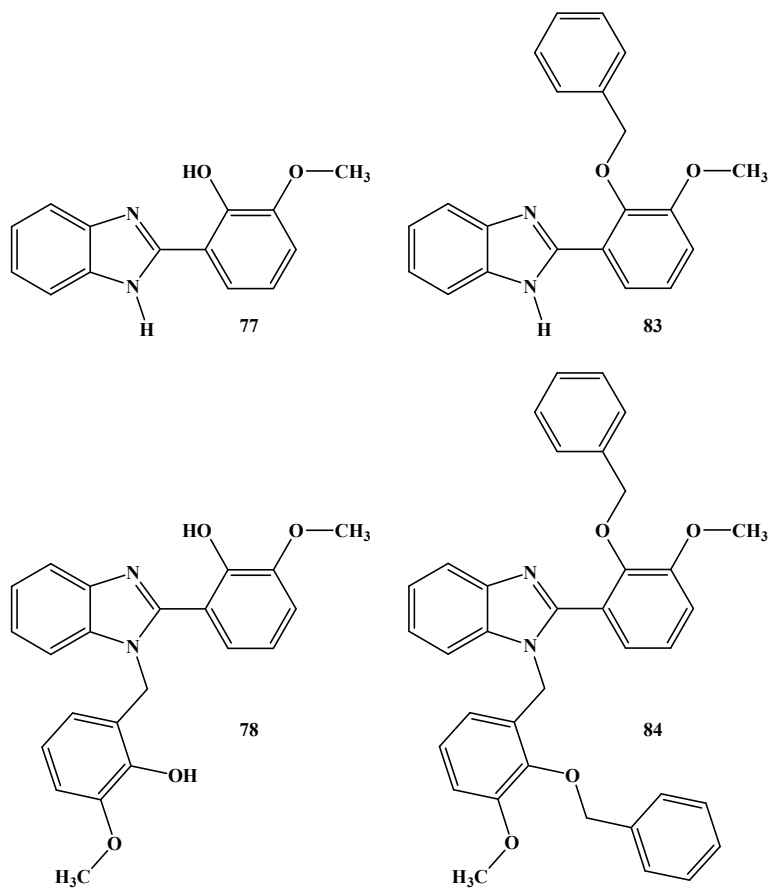
### 1.3 Scope of this work

In the current project, four types of different structures were targeted. 2-Benzyloxy-3-methoxy-benzaldehyde or benzyl *o*-vanillin **75**, two of 2-amino-*N*-benzylidene benzeneamines **76** and **82**, three of bis-Schiff bases **79**, **80** and **81** and four of benzimidazoles **77**, **78**, **83** and **84** were synthesized with modified methods and characterized by FTIR, HRMS, 1D and 2D NMR spectroscopy and X-ray crystallography (Figures 1.9-1.12).

Benzyl *o*-vanillin **75** was prepared to protect the hydroxyl group of *o*-vanillin, which was benzylated using modified preparation method. The comparison of the *o*-vanillin products and its derivative **75** reactions with *o*-phenylenediamine was studied. Both aldehydes *o*-vanillin and **75** were used to prepare benzimidazole derivatives **77**, **78**, **83** and **84** *via* amino benzeneamines intermediates **76** and **82**, respectively.

Figure 1.9: Structure of benzyl *o*-vanillin **75**.Figure 1.10: Structures of 2-amino-*N*-benzylidene benzeneamines **76** and **82**.

Bis-Schiff base **79** was also found as a main product from the reaction between *o*-vanillin with *o*-phenylenediamine, while both bis-Schiff bases **80** and **81** were prepared from the reaction of *o*-vanillin with *m*-phenylenediamine and *p*-phenylenediamine, respectively. The benzimidazoles **77**, **78**, **83** and **84** were evaluated as anti-proliferation with MTT assay.

Figure 1.11: Structures of bis-Schiff bases **79**, **80** and **81**.Figure 1.12: Structures of benzimidazoles **77**, **78**, **83** and **84**.

### 1.3.1 The objectives

The objectives of this work are listed as follows:

- (a) To synthesize 2-benzyloxy-3-methoxybenzaldehyde, **75**.
- (b) To synthesize both 2-amino-*N*-benzylidene benzeneamines **76** and **82**.
- (c) To synthesize bis-Schiff bases, **79**, **80** and **81**.
- (d) To synthesize the benzimidazole derivatives, **77**, **78**, **83** and **84**.
- (e) To elucidate the structures of the synthesized compounds using FTIR, HRMS, NMR and X-ray crystallography techniques (if applicable).
- (f) To evaluate the benzimidazoles **77**, **78**, **83** and **84** as anti-proliferation with MTT assay.

## CHAPTER TWO

## MATERIALS AND METHODS

## 2.1 Chemicals

The chemicals that were used throughout the project are listed as follows, which were used without further purification:

Acetone (AR grade)	Riedel-de Haën, Germany.
Acetone-D6 (acetone- $d_6$ ) contains 0.03 v/v % TMS (for NMR spectroscopy)	Sigma-Aldrich, USA.
Anhydrous Magnesium sulfate	Fluka Chemika, Switzerland.
Benzyl bromide	Fluka Chemika, Switzerland.
Chloroform ( $\text{CHCl}_3$ ), (AR grade)	Riedel-de Haën, Germany.
Chloroform-D ( $\text{CDCl}_3$ ) contains 0.03 v/v % TMS (for NMR spectroscopy)	Sigma-Aldrich, USA.
Dichloromethane (DCM), (AR grade)	Riedel-de Haën, Germany.
Dichloromethane-D2 ( $\text{CD}_2\text{Cl}_2$ ) contains 0.03 v/v % TMS (for NMR spectroscopy)	Sigma-Aldrich, USA.
Diethyl ether	Riedel-de Haën, Germany.
Dimethyl sulfoxide (DMSO)	Sigma-Aldrich, USA.
Dulbecco's Modified Eagle Medium (DMEM)	Gibco, Life technology, UK.
Ethanol	Riedel-de Haën, Germany.
HCT-116	ATCC, Rockville, MD, USA.
Heat inactivated fetal calf serum (HIFCS)	Sigma-Aldrich, Germany.
<i>n</i> -Hexane	Riedel-de Haën, Germany.
2-Hydroxy-3-methoxybenzaldehyde ( <i>o</i> -vanillin)	Sigma-Aldrich, USA.
McCoy's (growth medium)	Gibco, Life technology, UK.